J. Fluid Mech. (1981), *vol.* 103, *pp.* 413–442
Printed in Great Britain

Linearized analysis of the three-dimensional compressible flow through a rotating annular blade row

By JOHN A. LORDI AND GREGORY F. HOMICZ

Aerodynamic Research Department,
Calspan Advanced Technology Center,
Buffalo, New York

(Received 27 August 1979 and 7 April 1980)

Linearized solutions for the flow field of a rotating blade row in an infinitely long annular duct are reviewed. An isolated rotor is assumed to operate in a uniform axial flow so that the disturbance field is steady in a blade-fixed co-ordinate system. Both three-dimensional and compressibility effects are included, but attention is confined to subsonic flows. Previously published source-flow solutions omitted a term which affected the thickness part of the rotor flow field constructed from them. Corrected source and rotor-thickness solutions are given, and then the source or monopole solution is used to form a pressure dipole solution. The rotor-loading contribution to the flow field is found by superposition of the revised dipole solutions. The present version of the dipole representation of the steady-loading field is shown to be equivalent to an existing vortex representation, but different from an existing dipole representation. The behaviour of the blade-surface pressure and velocity distributions is described for both the thickness and loading cases. Sample numerical evaluations of the surface quantities are presented.

1. Introduction

Increased emphasis on the reduction of the size, weight, and noise output of axial-flow turbomachinery demands improved understanding of the flow through high-speed fan and compressor blade rows. As more detailed questions are asked about modern blade-row performance, the essentially three-dimensional character of the flow takes on increased importance. The task of calculating the fully nonlinear, three-dimensional, viscous flow through interacting blade rows is a formidable one indeed. Consequently, some approximations are required in order to obtain a tractable model, the most familiar being the idealization of inviscid flow through a two-dimensional cascade. A linearized analysis of the steady, inviscid, three-dimensional flow through an isolated rotor contains important features not present in the corresponding two-dimensional cascade approximation. For example, though restricted to lightly loaded, thin blades, it does include disturbances induced by the trailing vortex wakes which result from spanwise variations in the blade circulation.

The small-perturbation approach to three-dimensional compressor flows was begun by McCune (1958*a*, *b*) who, in the spirit of linearized wing theory, separated the thickness and loading contributions to the rotor disturbance field. In his original papers, McCune treated the thickness problem for the subsonic, transonic, and supersonic flow regimes. Later, Okurounmu & McCune (1970, 1974) employed a vortex represen-

0022-1120/81/4607-3010 $02.00

tation of the blade row to solve the indirect lifting problem, defined here to be that in which the disturbance field, along with the blade geometry needed to produce it, are determined from a prescribed distribution of blade loading.

While the thickness and loading contributions to the rotor disturbance field can be treated separately in a linearized analysis, they are not entirely independent. In order that there be no loading contribution to the flow field associated with a given distribution of blade thickness, this thickness must be distributed about an unknown camber line. The camber lines required for the rotor to be unloaded must be determined as part of the solution to the thickness problem, in much the same way as the camber lines corresponding to a specified loading distribution are computed. Erickson, Lordi & Rae (1971) presented results for thickness-induced camber lines at high subsonic tip speeds. They also have computed the camber lines required to produce given loading distributions, as have Okurounmu & McCune (1974).

Recently, linearized analyses of three-dimensional compressor flow fields have been concerned with lifting-surface calculations for both steady and unsteady flows. In contrast to the indirect loading problem for steady flow, the direct problem refers to the situation where the blade incidence and camber lines are given, and the resulting blade loading must be determined. The solution of the direct problem, together with the solution of the thickness problem, permits computation of the aerodynamic and acoustic performance for a rotor row of given geometry at specified operating conditions. In addition to a predictive capability for steady flow at off-design conditions, the successful analysis of the direct lifting-surface problem provides a basis for examining three-dimensional flows which are unsteady in rotor co-ordinates. The task of calculating the unsteady blade loading produced by a prescribed upwash distribution or small-amplitude blade motion is closely analogous to the evaluation of the steady loading corresponding to given blade camber lines.

Progress on the direct loading problem in steady flow has been reported by other investigators. McCune & Dharwadkar (1972) have obtained a solution using a lifting-line approximation. Namba (1972) has reported a direct lifting-surface analysis, including some numerical results. In addition, Namba and Salaun (1974) have extended the lifting-surface analyses to flows that are unsteady in rotor co-ordinates, and have presented results for the response of the rotor to inflow distortions (Namba 1977), and for the problem of blade flutter (Namba 1976; Salaun 1976).

The present paper is an outgrowth of our own work (Homicz & Lordi 1979) on the direct lifting-surface problem. In the course of deriving the governing integral equation for the blade loading, we had difficulty reconciling the different formulations for the rotor flow field. In their treatment of the loading contribution, Okurounmu & McCune (1974) use a vortex representation of the lifting surface; Namba (1972) uses a pressure-dipole approach. The disagreements encountered in the respective flow-field solutions prompted a complete review of the linearized analyses, and led to a revision of the fundamental source and dipole solutions. The purpose of this paper is to present this review and to resolve the discrepancies in the linearized solutions for the loading contribution to the steady flow through a compressor rotor. The rotor thickness contribution is discussed also, because it too is affected by the revised singularity solutions.

In § 2 the linearized equations for the three-dimensional, compressible flow through a rotor are reviewed, and a formal solution of them is obtained based on Green's theorem. In § 3, solutions are found for the disturbance fields of a point source of mass

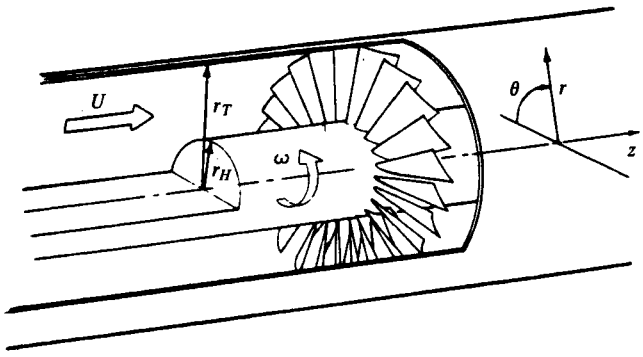

FIGURE 1. Blade geometry and blade-fixed co-ordinate system.

and a pressure dipole. Next, in §§ 4 and 5 respectively, these singularity solutions are used as Green's functions to determine the flow fields produced by rotor thickness and loading distributions. In § 6, the expressions for the flow-field quantities at the blade surfaces are presented and are shown to display the correct discontinuous behaviour across the blade surfaces and trailing vortex wakes. The equivalence of the pressure-dipole representation of the lifting surface and the vortex theory of Okurounmu & McCune (1970) is demonstrated in § 7. Results of sample calculations of the blade-surface quantities are described in § 8. Then the status of linearized solutions for the flow through a rotating blade row is summarized.

2. Derivation of model equations and Green's function solution

In this section, the linearized equations and a formal integral representation of their solution are developed for the flow through an isolated rotor row in an infinitely long annular duct. The key assumptions in the analysis are that the undisturbed axial velocity is uniform and subsonic, and that the disturbance field of the rotor is a small perturbation about the resulting helical inflow seen by an observer in blade-fixed co-ordinates. Both compressibility and three-dimensional effects are included. While not a fundamental restriction in the analysis, attention is confined to subsonic relative tip speeds. The required extensions to supersonic tip speeds are indicated by McCune (1958*a*, *b*) and by Okurounmu & McCune (1974). As a consequence of the linearization, the blade-surface boundary conditions can be separated into thickness and camber line contributions, and their associated flow-field solutions superimposed to find the overall disturbance field. This separation is effected by requiring the rotor blades to be locally unloaded in the thickness case and by assuming that the blades have vanishing thickness in the loading case.

The geometry of the blade-fixed co-ordinates is illustrated in figure 1 for a rotor rotating in the negative θ direction with angular velocity ω. The full nonlinear equations for the flow through such a blade row in a cylindrical co-ordinate system fixed to the rotor have been given by Wu (1952). These equations can be linearized by writing the velocity in blade-fixed coordinates as $\mathbf{W} = \mathbf{U}_R + \mathbf{v}$, where $\mathbf{U}_R$ is the undisturbed velocity, which has an axial component U, and a tangential component ωr; $\mathbf{v}$ is the perturbation velocity with components v_r, v_θ, v_z. The fluid pressure and

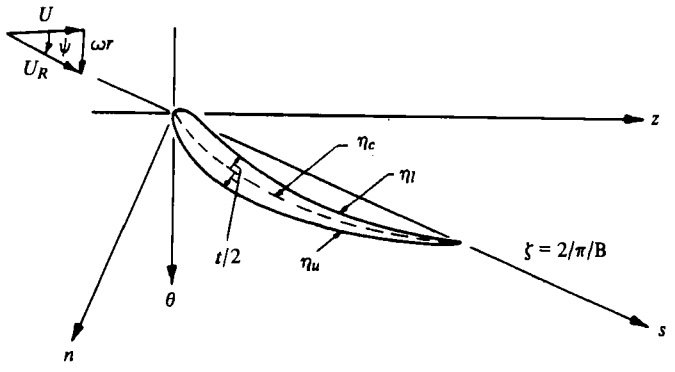

FIGURE 2. Blade surface geometry at fixed radius.

density are expanded in a similar way; the undisturbed quantities are denoted by p_∞ and ρ_∞, the perturbation quantities by p and ρ. Substituting these definitions into Wu's equations and linearizing the result by neglecting the products of perturbation quantities leads to the following vector forms of the steady flow continuity and momentum equations, to first order:

$$\mathbf{U}_R . \nabla\rho + \rho_\infty(\nabla . \mathbf{v}) = 0, \tag{1}$$

$$(\mathbf{v} . \nabla)\,\mathbf{U}_R + (\mathbf{U}_R . \nabla)\,\mathbf{v} + 2\omega(v_\theta \mathbf{e}_r - v_r \mathbf{e}_\theta) = -(1/\rho_\infty)\,\nabla p. \tag{2}$$

The momentum equation is easily written in component form for the cylindrical co-ordinates fixed to the blades. However, in the subsequent development of the rotor flow-field solution, it is convenient to work with co-ordinates along the undisturbed streamlines, and along the direction normal to both the streamline and radial directions. Unit vectors in these directions are denoted **s** and **n**, as illustrated in figure 2, and the respective velocity components are v_s and v_n. In the (r, s, n) co-ordinates, the momentum equations are

$$\rho_\infty U_R \partial v_r/\partial s = -\partial p/\partial r, \tag{3a}$$

$$\rho_\infty U_R \partial v_s/\partial s = -\partial p/\partial s, \tag{3b}$$

$$\rho_\infty U_R \partial v_n/\partial s = -\partial p/\partial n, \tag{3c}$$

where the directional derivatives $\partial/\partial s$ and $\partial/\partial n$ are related to the partial derivatives with respect to θ and z by

$$\frac{\partial}{\partial s} = \left(\frac{\omega}{U}\frac{\partial}{\partial\theta} + \frac{\partial}{\partial z}\right) \Big/ \left[1 + \left(\frac{\omega r}{U}\right)^2\right]^{\frac{1}{2}}, \tag{4a}$$

$$\frac{\partial}{\partial n} = \left(\frac{1}{r}\frac{\partial}{\partial\theta} - \frac{\omega r}{\partial}\frac{\partial}{\partial z}\right) \Big/ \left[1 + \left(\frac{\omega r}{U}\right)^2\right]^{\frac{1}{2}}. \tag{4b}$$

These forms of the linearized momentum equations are useful in relating results for the pressure and velocity fields. For subsonic flow, where disturbances decay far upstream, (3*b*) can be integrated along the streamlines to obtain

$$p = -\rho_\infty U_R v_s. \tag{5}$$

The normal momentum equation (3*c*) plays a central role in the direct lifting-surface theory. It contains the upwash velocity, v_n, which is related to the blade camber line in deriving the integral equation for the blade loading.

The set of governing equations is completed by introducing the assumption that the disturbance flow is isentropic, so that

$$p = a_\infty^2 \rho, \tag{6}$$

where a_∞ is the undisturbed sound speed. From this basic set of conservation equations, we can develop the governing equations for either the perturbation pressure or the velocity potential, the solutions of which can then be used to obtain the remaining flow-field quantities.

The governing equation for the perturbation pressure is derived by using (6) to eliminate the density in the linearized continuity and momentum equations. Then, combining $U_R \partial/\partial s$ of the continuity equation with the divergence of the momentum equation leads to

$$\nabla^2 p - \frac{U_R^2}{a_\infty^2} \frac{\partial^2 p}{\partial s^2} = 0. \tag{7}$$

The velocity potential satisfies the same governing differential equation. The linearized momentum equations indicate that the velocity components are proportional to the gradient of the integral of the pressure along the undisturbed streamlines. Accordingly, if a scalar velocity potential, defined such that $\mathbf{v} = \nabla\phi$, is introduced into (1) and (3*b*), the results may be combined with (6) to obtain

$$\nabla^2 \phi - \frac{U_R^2}{a_\infty^2} \frac{\partial^2 \phi}{\partial s^2} = 0. \tag{8}$$

The formal solution of the governing differential equation for ϕ (or p) is derived from Green's theorem, written for two scalar functions ϕ and G,

$$\int_S \left(G \frac{\partial \phi}{\partial \nu} - \phi \frac{\partial G}{\partial \nu} \right) dS = - \int_V (G \nabla^2 \phi - \phi \nabla^2 G)\, dV, \tag{9}$$

where the surface S encloses the volume V and $\boldsymbol{\nu}$ is the normal to the surface S directed into V. The following development, while carried out for the velocity potential, applies as well to the pressure perturbation.

The operator L is defined by writing (8) as $L\phi = 0$, and then the $\nabla^2\phi$ and $\nabla^2 G$ factors in Green's theorem are written in terms of L. Equation (9) becomes

$$\int_S \left(G \frac{\partial \phi}{\partial \nu} - \phi \frac{\partial G}{\partial \nu} \right) dS = - \int_V (GL\phi - \phi LG)\, dV - \int_V \left(GM_R^2 \frac{\partial^2 \phi}{\partial s^2} - \phi M_R^2 \frac{\partial^2 G}{\partial s^2} \right) dV, \tag{10}$$

where we have introduced the undisturbed relative Mach number in blade-fixed coordinates, $M_R = U_R/a_\infty$.

The second volume integral on the right-hand side can be rewritten as

$$\int_V \left(GM_R^2 \frac{\partial^2 \phi}{\partial s^2} - \phi M_R^2 \frac{\partial^2 G}{\partial s^2} \right) dV = \int_V M_R \frac{\partial}{\partial s} \left(GM_R \frac{\partial \phi}{\partial s} - \phi M_R \frac{\partial G}{\partial s} \right) dV. \tag{11}$$

In this form, the volume integral can be converted to a surface integral by applying the divergence theorem to the product of a scalar function and a vector, and the result used in (10) to obtain

$$\int_S \left(G\frac{\partial\phi}{\partial\nu} - \phi\frac{\partial G}{\partial\nu}\right) dS = -\int_V (GL\phi - \phi LG)\, dV + \int_S \boldsymbol{\nu}\cdot(\mathbf{A}\Phi)\, dS, \tag{12}$$

where

$$\Phi = GM_R\, \partial\phi/\partial s - \phi M_R\, \partial G/\partial s, \tag{13}$$

$$\mathbf{A} = M_R\mathbf{s}. \tag{14}$$

This relationship can be used to express the velocity potential in terms of surface integrals which bound the region of solution by the usual Green's function technique. The scalar function G in (12) is chosen to be the Green's function which is the solution to the equation

$$LG(\mathbf{r}, \mathbf{r}_0) = \delta(\mathbf{r} - \mathbf{r}_0) \tag{15}$$

where δ denotes the Dirac delta function and $\mathbf{r}$ and $\mathbf{r}_0$ denote the observation and source points. If the integrations in (12) are taken to be over the source co-ordinates, and within the region of interest $L_0\phi(\mathbf{r}_0) = 0$, then the following integral expression is obtained for the velocity potential:

$$\phi(\mathbf{r}) = \int_S \left[G(\mathbf{r}, \mathbf{r}_0)\frac{\partial\phi}{\partial\nu_0} - \phi(\mathbf{r}_0)\frac{\partial G}{\partial\nu_0}\right] dS_0 - \int_S [\boldsymbol{\nu}_0\cdot(\mathbf{A}\Phi)_0]\, dS_0. \tag{16}$$

The term $\phi(\mathbf{r})$ is the result of integrating $\phi(\mathbf{r}_0)\, L_0 G(\mathbf{r}, \mathbf{r}_0)$ over the volume, which requires that the Green's function determined from (15) also have the property

$$L_0 G(\mathbf{r}, \mathbf{r}_0) = \delta(\mathbf{r}_0 - \mathbf{r}). \tag{17}$$

An alternative approach to the integration over the region containing the singular point is to exclude this point from the volume integral by surrounding it with a vanishingly small surface. Then the functions ϕ and G are continuous and differentiable throughout the region of interest, and the volume integral in (12) vanishes. However, there would then be a contribution from the integration over the surface enclosing the point $\mathbf{r} = \mathbf{r}_0$. It has been demonstrated, using the Green's function determined in the subsequent section, that the integral over such a surface yields the same result as the volume integral over the delta function. That demonstration is quite lengthy and so the generalized function approach is used to handle point singularities where the presentations are thereby shortened.

In the present application, the surfaces over which the integrations must be done in (16) include the blade surfaces, the duct walls, and the surfaces normal to the duct axis at large distances upstream and downstream of the blade row. The evaluation of the surface integrals is simplified considerably through the use of a Green's function which satisfies the same boundary conditions at the duct walls as the velocity potential. Then the velocity potential for a rotor can be found by superimposing the solutions for singularities which are distributed only over the blade surfaces. In the next section,

the solutions for a point source of mass and a pressure dipole are found for the ducted geometry.

3. Mass source and pressure dipole solutions

The governing differential equation for the velocity potential given in (8) can be expressed in cylindrical co-ordinates by using (4*a*). Then, the velocity potential due to a source located at r_0, θ_0, z_0 in a rotating reference frame and having a mass addition rate of $\rho_\infty Q$ satisfies the equation

$$\beta^2\frac{\partial^2\phi}{\partial z^2}+\frac{1}{r}\frac{\partial}{\partial r}\left(r\frac{\partial\phi}{\partial r}\right)+\left(\frac{1}{r^2}-\frac{\omega^2}{a_\infty^2}\right)\frac{\partial^2\phi}{\partial\theta^2}-\frac{2\omega M}{a_\infty}\frac{\partial^2\phi}{\partial z\,\partial\theta}=Q\delta(z-z_0)\,\delta(\theta-\theta_0)\,\delta(r-r_0)/r, \tag{18}$$

where M is the Mach number based on the undisturbed axial velocity (U/a_∞) and $\beta^2 = 1-M^2$. In this form the homogeneous equation is separable and, as originally shown by McCune (1958*a*), it possesses the following eigenfunction solutions when the boundary condition of no flow through the walls is enforced:

$$\phi_H = \exp(in\theta)\exp\left(in\frac{M^2}{\beta^2}\frac{\omega z}{U}\pm\lambda_{nk}\frac{\omega z}{U}\right)R_{nk}(K_{nk}\sigma). \tag{19}$$

The quantity R_{nk} is a normalized combination of the Bessel and Neumann functions of order n as described by McCune (1958*a*). Also $\sigma = r/r_T$ and K_{nk} is the kth eigenvalue of the equations which result from the boundary condition that $\partial\phi/\partial r$ vanish at the duct walls. The eigenfunctions satisfy

$$R'_{nk}(h) = R'_{nk}(1) = 0. \tag{20}$$

The hub-to-tip radius ratio is $h = r_H/r_T$ and λ_{nk} is defined by

$$\lambda_{nk} = \frac{nU}{\omega r_T\beta^2}\left[\beta^2\left(\frac{K_{nk}}{n}\right)^2 - M_T^2\right]^{\frac{1}{2}}, \tag{21}$$

with $M_T = \omega r_T/a_\infty$. Transformed to duct-fixed co-ordinates, these homogeneous solutions represent the duct acoustic modes; equation (21) contains the so-called cut-off condition for the propagation of these modes. When $M_T > \beta(K_{nk}/n)$, λ_{nk} becomes imaginary and the solutions in (19) correspond to propagating waves. The cut-off condition can be stated approximately as requiring that the relative Mach number at the tip radius must be supersonic for the source to excite propagating modes. Here we restrict attention to the subsonic case where the modes decay with distance from the source.

In order to solve (18), the form of (19) suggests that we assume an expansion for ϕ of the form

$$\phi_s = \sum_{n=-\infty}^{\infty}\sum_{k=k_1}^{\infty}\phi_{nk}(z)\exp(in(\theta-\theta_0))\,R_{nk}(K_{nk}\sigma), \tag{22}$$

where ϕ_s will denote the solution for a mass source. Here $k_1 = 1$ for $n > 0$ but $k_1 = 0$ for $n = 0$ in order to include the non-trivial zero eigenvalue required to make the

zeroth-order Bessel functions a complete set. In addition we introduce the expansions of the delta functions in terms of the azimuthal and radial eigenfunctions:

$$\delta(\theta-\theta_0) = \frac{1}{2\pi}\sum_{n=-\infty}^{\infty} \exp\left(in(\theta-\theta_0)\right), \tag{23a}$$

$$\frac{\delta(r-r_0)}{r} = \frac{1}{r_T^2}\sum_{k=1}^{\infty} R_{nk}(K_{nk}\sigma_0)\, R_{nk}(K_{nk}\sigma), \quad n \neq 0, \tag{23b}$$

$$\frac{\delta(r-r_0)}{r} = \frac{2}{(1-h^2)\,r_T^2} + \frac{1}{r_T^2}\sum_{k=1}^{\infty} R_{0k}(K_{0k}\sigma_0)\, R_{0k}(K_{0k}\sigma), \quad n = 0. \tag{23c}$$

Substituting these expansions into (18), using the differential equation satisfied by the radial eigenfunctions,

$$\frac{1}{r}\frac{d}{dr}\left(r\frac{dR_{nk}}{dr}\right) + \left(\frac{K_{nk}^2}{r_T^2} - \frac{n^2}{r^2}\right) R_{nk} = 0, \tag{24}$$

and making use of the orthogonality properties of the azimuthal and radial eigenfunctions leads to

$$\beta^2\frac{d^2\phi_{nk}}{dz^2} - \frac{2in\omega M}{a_\infty}\frac{d\phi_{nk}}{dz} + \left(\frac{n^2\omega^2}{a_\infty^2} - \frac{K_{nk}^2}{r_T^2}\right)\phi_{nk} = \frac{QR_{nk}(\sigma_0)}{2\pi r_T^2}\,\delta(z-z_0), \tag{25}$$

where $R_{nk}(\sigma_0)$ is introduced as a shortened notation for $R_{nk}(K_{nk}\sigma_0)$. The solution of this equation for $\phi_{nk}(z)$ can be found using Fourier transform techniques. With the following transform definition

$$\overline{\phi}_{nk}(\xi) = \frac{1}{2\pi}\int_{-\infty}^{\infty} e^{-i\xi z}\,\phi_{nk}(z)\,dz, \tag{26}$$

taking the transform of (25), solving for $\overline{\phi}_{nk}$, and taking the inverse transform yields

$$\phi_{nk}(z) = -\frac{QR_{nk}(\sigma_0)}{4\pi^2 r_T^2\beta^2}\int_{-\infty}^{\infty} e^{i\xi(z-z_0)}\left[\xi^2 - \frac{2n\omega M}{\beta^2 a_\infty}\,\xi + \frac{1}{\beta^2}\left(\frac{K_{nk}^2}{r_T^2} - \frac{n^2\omega^2}{a_\infty^2}\right)\right]^{-1} d\xi. \tag{27}$$

The integral in (27) can be evaluated by residue theory, the roots of the denominator being

$$\xi_{nk}^{\pm} = \frac{n\omega M}{\beta^2 a_\infty} \pm i\frac{n}{\beta^2 r_T}\left[\beta^2(K_{nk}/n)^2 - (\omega r_T/a_\infty)^2\right]^{\frac{1}{2}}. \tag{28}$$

For $z > z_0$ the contour is closed in the upper half-plane and encloses the pole at $\xi = \xi_{nk}^+$; for $z < z_0$ the contour is closed in the lower half-plane and encloses the pole at $\xi = \xi_{nk}^-$. This procedure ensures that the solution decays rather than diverging for $z \to \pm\infty$ (or for supersonic tip speeds, corresponds to outward-moving waves).

The case $n = 0$, $k = 0$ deserves special attention. For these values of n and k the integrand in (27) has a second-order pole at $\xi = 0$. The contribution from this pole is included in the contour which encloses the upper half-plane (corresponding to $z > z_0$) and excluded from the contour enclosing the lower half-plane (corresponding to $z < z_0$). This choice is made on the grounds that there can be no steady perturbation

at upstream infinity. Evaluating the integrals for ϕ_{nk} and using the results in (22), the solution for the source potential is

$$\phi_s(\mathbf{r}, \mathbf{r}_0) = \frac{Q}{2\pi r_T^2 \beta^2}\left(\frac{2}{1-h^2}\right)(z-z_0)\,H(z-z_0) - \frac{Q}{4\pi\beta^2 r_T^2}\sum_{n=-\infty}^{\infty}\sum_{k=1}^{\infty}\frac{R_{nk}(\sigma_0)\,R_{nk}(\sigma)}{\omega\lambda_{nk}/U} \times \exp\left[in(\theta-\theta_0)+\frac{inM^2}{\beta^2}\frac{\omega}{U}(z-z_0)-\frac{\omega\lambda_{nk}}{U}|z-z_0|\right], \quad (29)$$

where $H(z-z_0)$ is the Heaviside step function.

The first term in the source solution has been omitted in previous treatments. Except for the presence of this term, the above result can be integrated in the radial direction to recover the line source solution which McCune (1958*a*, *b*) used to solve the rotor thickness problem. The omission of this term in the mass source (or pressure monopole) solution also affects the fluid doublet (or pressure dipole) solution. The implications that omitting this term from the source and dipole solutions have for the rotor thickness and loading problems are elaborated upon below where those solutions are presented.

Several checks were made on the revised source solution. The first test made on the solution for ϕ_s was to substitute it back into (18), and to verify that it was indeed the correct solution. In addition, the pressure and velocity fields associated with the mass source solution were obtained from the velocity potential, and it has been verified that the solution displays the properties of a mass source. The linearized expression for the mass flux through a small surface surrounding the source, when integrated over the surface, results in a value of $\rho_\infty Q$ for the rate of introduction of mass.

In addition to the demonstration of mass conservation for the above control volume, a similar check has been made for the control volume bounded by the walls and the surfaces normal to the duct axis at $z = \pm\infty$. It also has been shown that the results for the flow field of a point source satisfy the axial component of the linear and angular momentum balances for this latter control volume. The expressions for the mass addition rate, axial force, and axial component of the torque on the fluid in this control volume are given in appendix A. For the source solution, the expected results of $\rho_\infty Q$, $\rho_\infty UQ$, and $\rho_\infty \omega r_0^2 Q$ are obtained for these quantities.

The mass source solution can be used as the Green's function, and the solutions superimposed to represent the flow about a non-lifting rotor. The velocity potential of a fluid doublet could be obtained from that for a source in the conventional way, and then the flow field produced by rotor loading found by superposition of these doublet solutions. However, it is more convenient to treat the loading case in terms of the perturbation pressure because the blade boundary conditions are expressed in a simpler form and, further, integration over the blade wakes is avoided. Here the Green's function is interpreted as a pressure monopole and it, in turn, is differentiated to find the disturbance field of a pressure dipole. The pressure field of a lifting rotor can then be found by superposition of the pressure dipole solutions.

Since the rotor pressure field satisfies the same equation as the velocity potential, the solution for a pressure monopole is mathematically the same as the solution for a mass source. The corresponding dipole solution is found by differentiating the monopole solution. If the pressure monopole is to be used as the Green's function in the formal solution for the pressure, then the required orientation of the dipoles is normal

to the blade surfaces or, in the linearized analysis, to the undisturbed stream direction. For a dipole of strength D located at the point $\mathbf{r}_0$ and oriented in the positive $\mathbf{n}_0$ direction shown in figure 2, the pressure field p_D can be expressed as

$$p_D = D\,\partial G(\mathbf{r}, \mathbf{r}_0)/\partial n_0, \tag{30}$$

where $G(\mathbf{r}, \mathbf{r}_0)$ is the source (or monopole) solution given in (29) with unit strength. Performing the indicated operations in (30),

$$\begin{aligned} p_D = \frac{D}{4\pi\beta^2 r_T^2 [1+(\omega r_0/U)^2]^{\frac{1}{2}}} \Bigg\{ 2\left(\frac{\omega r_0}{U}\right)\left(\frac{2}{1-h^2}\right) H(z-z_0) + \sum_{n=-\infty}^{\infty} \sum_{k=1}^{\infty} \frac{R_{nk}(\sigma_0)\, R_{nk}(\sigma)}{\omega\lambda_{nk}/U} \\ \times \left[\frac{in}{r_0} - \frac{\omega^2 r_0}{U^2}\left(\frac{inM^2}{\beta^2}\right) + \frac{\omega^2 r_0}{U^2}\lambda_{nk}\,\mathrm{sgn}\,(z-z_0)\right] \\ \times \exp\left[in(\theta-\theta_0) + \frac{inM^2}{\beta^2}\frac{\omega}{U}(z-z_0) - \frac{\omega\lambda_{nk}}{U}|z-z_0|\right]\Bigg\}. \end{aligned} \tag{31}$$

As with the result for ϕ_s, this solution for p_D has been substituted into the governing differential equation to verify that it is the correct solution. Forming the quantity Lp_D yields the result

$$Lp_D = D\frac{\partial}{\partial n_0}[r_0^{-1}\,\delta(r-r_0)\,\delta(\theta-\theta_0)\,\delta(z-z_0)], \tag{32}$$

when the series expansions in (23) are used for the delta functions.

The velocity components associated with the dipole field are obtained by integrating the momentum equations (3) along the undisturbed streamlines. Consistent with our generalized-function approach in treating singular points, a delta-function body force is included in the momentum equations. Then, the resulting expressions for the velocities are valid everywhere in the duct, including points which lie on the streamline that passes through the dipole location. Otherwise, the expressions would not be valid in a small region enclosing this streamline.

The dipole exerts a force per unit volume on the fluid, $\mathbf{F}_D$, which is in the negative $\mathbf{n}$ direction and expressed by

$$\mathbf{F}_D = -\mathbf{n}Dr_0^{-1}\delta(r-r_0)\,\delta(\theta-\theta_0)\,\delta(z-z_0). \tag{33}$$

The streamwise velocity component is simply proportional to the pressure by (5), which was derived by integrating the streamwise momentum equation. Integrating the radial and normal momentum equations along the undisturbed streamlines yields

$$(v_r)_D = -\frac{1}{\rho_\infty U_R}\int_{-\infty}^{s} \frac{\partial p_D(s')}{\partial r}\,ds', \tag{34a}$$

$$(v_n)_D = -\frac{1}{\rho_\infty U_R}\int_{-\infty}^{s} \frac{\partial p_D(s')}{\partial n}\,ds' + \frac{1}{\rho_\infty U_R}\int_{-\infty}^{s} F_D(s')\,ds'. \tag{34b}$$

The expressions for $(v_r)_D$ and $(v_n)_D$ can both be written in terms of the integral of p_D along the undisturbed streamlines. The integration is done by expressing ds in terms

of dz, using the fact that along the undisturbed streamlines $\theta - \omega z/U$ and r remain constant. The result of integrating the expression for p_D along the streamlines is

$$\int_{-\infty}^{s} p_D(s')\,ds' = \frac{D(\omega r_0/U)}{2\pi\beta^2 r_T^2}\left[\frac{1+(\omega r/U)^2}{1+(\omega r_0/U)^2}\right]^{\frac{1}{2}}\left(\frac{2}{1-h^2}\right)(z-z_0)\,H(z-z_0)$$
$$+\frac{D}{4\pi\beta^2 r_T^2}\left[\frac{1+(\omega r/U)^2}{1+(\omega r_0/U)^2}\right]^{\frac{1}{2}}\sum_{n=-\infty}^{\infty}\sum_{k=1}^{\infty}\frac{R_{nk}(\sigma_0)\,R_{nk}(\sigma)}{\omega\lambda_{nk}/U}\exp\left(in(\theta-\theta_0)\right)$$
$$\times\left\{\left[\frac{1+(\omega r_0/U)^2}{\omega r_0/U}\right]\frac{2in\lambda_{nk}H(z-z_0)}{(n^2/\beta^4)+\lambda_{nk}^2}\right.$$
$$+\frac{\left[\dfrac{in}{r_0}-\dfrac{\omega^2 r_0}{U^2}\left(\dfrac{inM^2}{\beta^2}\right)+\dfrac{\omega^2 r_0}{U^2}\lambda_{nk}\operatorname{sgn}(z-z_0)\right]}{\dfrac{\omega}{U}\left[\dfrac{in}{\beta^2}-\lambda_{nk}\operatorname{sgn}(z-z_0)\right]}$$
$$\left.\times\exp\left[\frac{inM^2}{\beta^2}\frac{\omega}{U}(z-z_0)-\frac{\omega\lambda_{nk}}{U}|z-z_0|\right]\right\}. \tag{35}$$

The expressions given for the velocity components in (34) have been formed and, using the formulae given in appendix A, it has been verified that the dipole solution possesses the appropriate properties of not introducing any mass into the flow, and exerting a force D on the fluid. In the next two sections, the source and dipole solutions in (29) and (31) are used as the Green's functions to construct the flow field produced by a rotor with distributed thickness and loading.

4. Flow field of a non-lifting rotor (thickness problem)

In the previous two sections, the foundation has been laid to develop the solution for the thickness contribution to the flow field of a rotor in an annular duct. The source solution given in (29) can be used, with unit strength, as the Green's function, $G(\mathbf{r}, \mathbf{r}_0)$, in the integral representation of the velocity potential in (16). The integrations in (16) must be done over the following surfaces: (i) the duct walls, (ii) the surfaces normal to the duct axis at large distance from the rotor, and (iii) the blade surfaces. Along the inner and outer duct walls the boundary condition on $\phi(\mathbf{r}_0)$ is that the normal derivative vanish corresponding to no flow through the walls. Since the Green's function we have found satisfies the same boundary condition, the first integral in (16) vanishes for this surface. For the outer wall $\boldsymbol{\nu}_0 = -\mathbf{e}_r$ while for the inner wall $\boldsymbol{\nu}_0 = \mathbf{e}_r$. From (14) we see that $\boldsymbol{\nu}_0 . \mathbf{A} = 0$ along both the inner and outer walls, and so the second integral in (16) also vanishes at the duct walls.

For the surfaces normal to the duct axis at $z_0 \to +\infty$ and $z_0 \to -\infty$, $\boldsymbol{\nu}_0$ is $-\mathbf{e}_z$ and $+\mathbf{e}_z$ respectively. Over these two surfaces the sum of the two integrals vanishes because of the properties of the integrands. Consider the integrand at $z_0 \to +\infty$ first. In this case $z < z_0$ and so all the terms in $G(\mathbf{r}, \mathbf{r}_0)$ and its derivatives decay exponentially. Since $\phi(\mathbf{r}_0)$ and its derivatives must be bounded, the integrand vanishes as $z_0 \to +\infty$. Next, consider the integrand evaluated at $z_0 \to -\infty$. Here $z > z_0$ and the $n = 0, k = 0$ term

contributes to both G and $\partial G/\partial z_0$; the remaining terms in G, $\partial G/\partial\theta_0$ and $\partial G/\partial z_0$ decay exponentially. For subsonic flow, ϕ and the velocity components obtained from its derivatives are required to vanish far upstream of the blade row. Note that G diverges linearly as $z_0 \to -\infty$ and so the velocity field must fall off faster than this in order for the integrand to vanish. We shall see that the velocity field decays exponentially upstream of the rotor. Hence, the integrands vanish for $z_0 \to -\infty$ also.

In the linearized analysis, the blade row is assumed to make only a slight perturbation of the free-stream flow. Consistent with this assumption, the blade surface boundary conditions are applied along the undisturbed stream direction. In this approximation, the normals to the upper and lower blade surfaces are, respectively, $\boldsymbol{\nu}_0 = \pm\mathbf{n}_0 = \pm(\cos\psi_0\,\mathbf{e}_\theta - \sin\psi_0\,\mathbf{e}_z)$, where $\psi_0 = \tan^{-1}(\omega r_0/U)$. It can be seen that $\boldsymbol{\nu}_0 . \mathbf{A}$ vanishes and thus, in the linearized approximation, the second integral in (16) contains no contribution from the blade surfaces.

The separation of the rotor flow field into the thickness and loading contributions is made by prescribing that there be no pressure difference across the blade surfaces in the thickness case, or that the blades are locally unloaded. If the pressure is continuous across the blade surface, then v_s and ϕ are also. Hence, because of the opposite signs of $\partial G/\partial\nu_0$ on the upper and lower surfaces, only the part of the integrand containing $G\,\partial\phi/\partial\nu_0$ contributes to the integration over the blade surfaces. Thus, the expression for ϕ has been reduced to

$$\phi(\mathbf{r}) = \int_{S_B} G(\mathbf{r}, \mathbf{r}_0)\,\Delta(\partial\phi/\partial n_0)\,dS_B, \tag{36}$$

where S_B denotes the surface area of the rotor blades projected on the undisturbed stream surface, and $\Delta(\partial\phi/\partial n_0)$ represents the difference in normal velocity across each blade surface. This expression is the same as the familiar result in isolated airfoil theory that the effects of wing thickness can be represented by the superposition of sources whose strength is equal to the discontinuity in v_n at each point.

The linearized form of the blade boundary conditions is

$$v_n^u = U_R\,\partial\eta_u/\partial s, \quad v_n^l = U_R\,\partial\eta_l/\partial s, \tag{37}$$

where η_u and η_l are the distances to the upper and lower surfaces, measured normal to the undisturbed stream direction $\mathbf{s}$. The quantities η_u and η_l can be expressed in terms of a blade thickness and a blade incidence plus camber line in the conventional way, as illustrated in figure 2. However, for a rotor, the blade thickness and camber are not independent because, as noted earlier, in order for the blades to be unloaded they must be cambered to account for loadings which would otherwise be induced by blade interference effects. If $t(s,r)$ represents $\eta_u(s,r) - \eta_l(s,r)$, then

$$\begin{aligned} \eta_u(s,r) &= \eta_c(s,r) + \tfrac{1}{2}t(s,r), \\ \eta_l(s,r) &= \eta_c(s,r) - \tfrac{1}{2}t(s,r), \end{aligned} \tag{38}$$

where $\eta_c(s,r)$ is the camber line, which consists of two parts, a thickness part and a loading part. The discontinuity in the normal velocity across the blade surface is then related to the thickness distribution by

$$\Delta v_n = U_R\,\partial t/\partial s. \tag{39}$$

For a rotor with B equally spaced blades, the blades lie on the surfaces

$$\zeta = 2j\pi/B, \quad j = 0, 1, \ldots, B-1,$$

where ζ is the helical variable which is defined by

$$\zeta = \theta - \omega z/U. \tag{40}$$

The element of blade area in the constant-ζ surface is

$$dS_B = [1+(\omega r_0/U)^2]^{\frac{1}{2}}\, dr_0\, dz_0. \tag{41}$$

Expressed in the r, ζ, z co-ordinates, the velocity potential is

$$\phi(r,\zeta,z) = \sum_{j=0}^{B-1} \int_{r_H}^{r_T} \Delta v_n(r_0,z_0)\, G(r,\zeta,z;r_0,\zeta_0 = 2j\pi/B, z_0)\, [1+(\omega r_0/U)^2]^{\frac{1}{2}}\, dz_0\, dr_0, \tag{42}$$

where the blade leading edges are located at $z_0 = 0$ and, while not crucial to the ensuing analysis, it is assumed that the axial projection of the blade chord is a constant, c_a. Introducing the expressions for Δv_n and G (or ϕ_s), and performing the summation over the number of blades by using the identity

$$\sum_{j=0}^{B-1} e^{-in(2j\pi/B)} = \begin{cases} 0, & n \neq mB, \\ B, & n = mB, \end{cases} \tag{43}$$

where m is an integer, the result for the velocity potential becomes

$$\begin{aligned} \phi(r,\zeta,z) = \frac{BU}{2\pi\beta^2 r_T^2} \int_{r_H}^{r_T} \int_0^{c_a} \Bigg\{ \left(\frac{2}{1-h^2}\right) (z-z_0)\, H(z-z_0) \\ - \frac{1}{2} \sum_{m=-\infty}^{\infty} \sum_{k=1}^{\infty} \frac{R_{mBk}(\sigma_0)\, R_{mBk}(\sigma)}{\omega\lambda_{mBk}/U} \exp\left[imB\zeta + \Lambda^{\pm}_{mBk}(z-z_0)\right] \Bigg\} \\ \times \frac{\partial}{\partial z_0}[t(z_0,r_0)]\, [1+(\omega r_0/U)^2]^{\frac{1}{2}}\, dz_0\, dr_0. \end{aligned} \tag{44}$$

We have introduced the notation

$$\Lambda^{\pm}_{mBk}(z,z_0) = \frac{\omega}{U}\left[\frac{imB}{\beta^2} - \lambda_{mBk}\, \mathrm{sgn}\,(z-z_0)\right] \tag{45}$$

with the + sign applicable for $z > z_0$, or $\mathrm{sgn}\,(z-z_0) = +1$.

Having this solution for the velocity potential, the other flow-field variables can be found by taking the appropriate derivatives. The results for the velocity components are given in terms of v_s, v_n, and v_r, which are related to ϕ by

$$v_s = \partial\phi/\partial s = [1+(\omega r/U)^2]^{-\frac{1}{2}} \left.\frac{\partial\phi}{dz}\right|_{r,\zeta}, \tag{46a}$$

$$v_n = \partial\phi/\partial n = \frac{1}{r}[1+(\omega r/U)^2]^{\frac{1}{2}} \left.\frac{\partial\phi}{\partial\zeta}\right|_{r,z} - \frac{\omega r}{U} v_s, \tag{46b}$$

$$v_r = \partial\phi/\partial r. \tag{46c}$$

The pressure is simply proportional to v_s by (5). The resulting expressions for the velocity components are

$$\begin{aligned} \begin{bmatrix} v_s \\ v_n \\ v_r \end{bmatrix} = \frac{BU\cos\psi}{2\pi\beta^2 r_T^2} \int_{r_H}^{r_T} \int_0^{c_a} \Bigg\{ \begin{bmatrix} u \\ v \\ w \end{bmatrix} - \frac{1}{2} \sum_{m=-\infty}^{\infty} \sum_{k=1}^{\infty} \frac{R_{mBk}(\sigma)\, R_{mBk}(\sigma_0)}{\omega\lambda_{mBk}/U} \\ \times \begin{bmatrix} U_{mk} \\ V_{mk} \\ W_{mk} \end{bmatrix} \exp\left[imB\zeta + \Lambda^{\pm}_{mBk}(z-z_0)\right] \Bigg\} \frac{\partial t}{\partial z_0} \frac{dz_0\, dr_0}{\cos\psi_0}, \end{aligned} \tag{47}$$

where

$$u = \left(\frac{2}{1-h^2}\right) H(z-z_0), \quad v = -u\tan\psi, \quad w = 0,$$

$$U_{m,k} = \Lambda^{\pm}_{mBk},$$

$$V_{m,k} = \frac{imB}{r} - \frac{\omega^2 r}{U^2}\left[imB\frac{M^2}{\beta^2} - \lambda_{mBk}\,\mathrm{sgn}\,(z-z_0)\right],$$

$$W_{m,k} = \frac{R'_{mBk}(\sigma)}{R_{mBk}(\sigma)}\frac{K_{mBk}}{r_T\cos\psi}. \tag{48}$$

These results for the thickness contribution to the rotor flow field are valid throughout the duct. The factors u and v derive from the term omitted in the source solution in previous treatments and their impact on evaluations of these expressions will be discussed in § 6.

5. Flow field of a lifting rotor (loading problem)

The determination of the pressure field produced by a lifting rotor closely parallels the solution procedure for the velocity potential in the thickness problem. The Green's function is the same, though now its interpretation is in terms of a pressure monopole. The formal solution for p is identical with that given in (16) for ϕ, except for the replacement of ϕ with p. In addition, both of the integrations over the duct walls and the surfaces at $z_0 = \pm\infty$ vanish as before, as does the integration of $\boldsymbol{\nu}.(\mathbf{A}\Phi)$ over the blade surfaces. The remaining integral over the blade surfaces distinguishes the lifting case from the thickness case. Here the magnitude of $\partial p/\partial n_0$ is the same on both sides of the blades because v_n must be continuous. Since the normals to the upper and lower surfaces lie in opposite directions and $G(\mathbf{r},\mathbf{r}_0)$ is continuous across the blades, the integral of $G\,\partial p/\partial \nu_0$ over the blade surfaces vanishes. Thus the integral representation of the solution for the pressure field reduces to

$$p(\mathbf{r}) = \int_{S_B} \Delta p(\mathbf{r}_0)\,\partial G/\partial n_0\, dS_B, \tag{49}$$

where

$$\Delta p \equiv p(r_0, z_0, \zeta_0 = 2\pi j^-/B) - p(r_0, z_0, \zeta_0 = 2\pi j^+/B) \tag{50}$$

so that Δp is defined as a positive number.

If we substitute the pressure dipole solution (equation (31)) with unit strength for $\partial G/\partial n_0$ and, exactly as was done for ϕ in the thickness problem, carry out the summation over the number of blades, we get the following result for the pressure field of the rotor

$$p = \frac{\omega B}{2\pi\beta^2 U}\int_0^{c_a} \overline{\Delta p}(z_0)\,H(z-z_0)\,dz_0$$

$$+ \frac{B}{4\pi\beta^2 r_T^2}\int_{r_B}^{r_T}\int_0^{c_a} \sum_{m=-\infty}^{\infty}\sum_{k=1}^{\infty} \frac{R_{mBk}(\sigma)\,R_{mBk}(\sigma_0)}{\omega\lambda_{mBk}/U}$$

$$\times \exp\left[imB\zeta + \Lambda^{\pm}_{mBk}(z-z_0)\right] V_{m,k}(r_0, z, z_0)\,\Delta p(r_0, z_0)\,dz_0\,dr_0, \tag{51}$$

where we have introduced

$$\overline{\Delta p}(z_0) = \frac{2}{1-h^2}\int_h^1 \Delta p(r_0, z_0)\,\sigma_0\,d\sigma_0 \tag{52}$$

and the quantities $\Lambda^{\pm}_{mBk}$ and $V_{m,k}$ are defined in (45) and (48).

The first property of this solution to be examined is the limiting pressure rise between points far upstream and far downstream of the blade row. Since for subsonic flow the solution decays as $z \to -\infty$, the limiting value of the static pressure rise is simply the limiting value of p for $z \to +\infty$. All terms except the first decay and so

$$p(z \to \infty) = \frac{\omega B}{2\pi\beta^2 U}\int_0^{c_a} \overline{\Delta p}(z_0)\,dz_0. \tag{53}$$

This result agrees with that obtained from the vortex theory of Okurounmu & McCune (1970). In the present formulation its origin is in the $n = 0, k = 0$ term in the dipole solution. Namba (1972) reports a limiting static pressure rise which differs from (53) in two respects. First of all, he finds a non-vanishing pressure perturbation for $z \to -\infty$. Also, his result contains a 'scale factor' which introduces an additional radial dependence into the integrations over radius in (51) and (53). While this scale factor approaches unity in the two-dimensional limit of high hub-to-tip ratios h, its radial variation is significant for lower values of h. For example, for a tip stagger angle of 45°, it varies by a factor of 2–4, between the hub and the tip for h in the range of 0·4 to 0·6. Based on the tests we have made on the solutions, we have concluded that this factor should not be present.

In the pressure dipole representation of the blade row, the velocity field must be found by integrating the momentum equations along the undisturbed stream direction. The streamwise velocity perturbation v_s is found from (5). If $\partial p/\partial n$ is expressed in terms of the derivatives $[\partial/\partial z]_{\zeta,r}$ and $[\partial/\partial\zeta]_{z,r}$ then integration of the normal momentum equation (3c) along the undisturbed streamlines yields

$$v_n = \left(\frac{\omega r}{U}\right)\frac{p}{\rho_\infty U_R} - \frac{1}{\rho_\infty U_R}\frac{1}{r}[1+(\omega r/U)^2]\frac{\partial I}{\partial\zeta} + \frac{1}{\rho_\infty U_R}[1+(\omega r/U)^2]^{\frac{1}{2}}\int_{-\infty}^{z} F_B(r,\zeta,z')\,dz', \tag{54}$$

where $I(r,\zeta,z)$ is defined by

$$I(r,\zeta,z) = \int_{-\infty}^{z} p(r,\zeta,z')\,dz' \tag{55}$$

and z' is a dummy variable of integration. In keeping with the generalized function approach to the singularities, a body-force term representing the blade forces F_B has been included. Since this force acts normal to the undisturbed stream direction in the linearized theory, it appears only in the v_n expression. This contribution to v_n is

$$\frac{1}{\rho_\infty U}\int_{-\infty}^{z} F_B\,dz' = -\frac{[1+(\omega r/U)^2]}{\rho_\infty U_R r}\sum_{j=0}^{B-1}\delta(\zeta - 2j\pi/B)\int_0^{c_a}\Delta p(r,z')\,H(z-z')\,dz', \tag{56}$$

where we have accounted for the fact that the blades are located on the surfaces $\zeta = 2j\pi/B$ between the axial stations $z = 0$ and $z = c_a$. As we shall see, this term will be cancelled by other terms in v_n. For now the remaining terms in v_n will be designated

v_n'. After evaluating the integral of the pressure indicated in (55), the result can be combined with that for p according to (54) in order to obtain v_n':

$$v_n' = \frac{\omega B}{2\pi\beta^2 U}\frac{\omega r/U}{\rho_\infty U_R}\int_0^{c_a}\overline{\Delta p}(z_0)\,H(z-z_0)\,dz_0$$
$$+\frac{B}{2\pi\beta^2 r_T^2\rho_\infty U_R}\left[\frac{1+(\omega r/U)^2}{\omega r/U}\right]\int_{r_H}^{r_T}\int_0^{c_a}\sum_{m=-\infty}^{\infty}\sum_{k=1}^{\infty}R_{mBk}(\sigma)\,R_{mBk}(\sigma_0)\,e^{imB\zeta}$$
$$\times\left[\frac{(mB)^2}{(mB/\beta^2)^2+\lambda_{mBk}^2}\right]\left[\frac{1+(\omega r_0/U)^2}{\omega r_0/U}\right]H(z-z_0)\,\Delta p(r_0,z_0)\,dz_0\,dr_0$$
$$+\frac{B}{4\pi\beta^2 r_T^2\rho_\infty U_R}\int_{r_H}^{r_T}\int_0^{c_a}\sum_{m=-\infty}^{\infty}\sum_{k=1}^{\infty}\frac{R_{mBk}(\sigma)\,R_{mBk}(\sigma_0)}{\omega\lambda_{mBk}/U}\,e^{imB\zeta}\,V_{m,k}(r_0,z,z_0)$$
$$\times\left\{\frac{\omega r}{U}-\frac{imB}{\Lambda_{mBk}^{\pm}}\left[\frac{1}{r}(1+\omega^2 r^2/U^2)\right]\right\}\exp\left[\Lambda_{mBk}^{\pm}(z-z_0)\right]\Delta p(r_0,z_0)\,dz_0\,dr_0. \tag{57}$$

The expression for v_r which results from integrating the radial momentum equation (3a) is

$$v_r = -\frac{1}{\rho_\infty U}\frac{\partial I}{\partial r}, \tag{58}$$

which, upon using the result for I, is

$$v_r = -\frac{B}{4\pi\beta^2 r_T^2\rho_\infty U}\int_{r_H}^{r_T}\int_0^{c_a}\sum_{m=-\infty}^{\infty}\sum_{k=1}^{\infty}\frac{R'_{mBk}(\sigma)\,R_{mBk}(\sigma_0)}{\omega\lambda_{mBk}/U}\left(\frac{K_{mBk}}{r_T}\right)e^{imB\zeta}$$
$$\times\left\{2imB\lambda_{mBk}H(z-z_0)\left[\frac{1+(\omega r_0/U)^2}{\omega r_0/U}\right][(mB/\beta^2)^2+\lambda_{mBk}^2]^{-1}+\frac{V_{m,k}(r_0,z,z_0)}{\Lambda_{mBk}^{\pm}}\right.$$
$$\left.\times\exp\left[\Lambda_{mBk}^{\pm}(z-z_0)\right]\right\}\Delta p(r_0,z_0)\,dz_0\,dr_0. \tag{59}$$

Particular note should be paid to those terms in v_n and v_r which do not decay downstream of the rotor. These terms, which are present within the blade row and downstream of it, represent the contribution of the trailing vortex wakes to the velocity field. The flow field produced by these wakes has a helical pattern and, as a consequence of the linearization, the wakes coincide with the undisturbed stream surfaces on which the blades lie. There are no wake terms in p or v_s, which should be continuous across these surfaces.

6. Behaviour of the velocity components at the blade surfaces

Many applications of the foregoing analyses require the evaluation of the blade-surface velocity components or pressure distribution for which expressions are derived in this section. The equations given above for the disturbance velocity fields contain doubly infinite series expansions in the duct eigenfunctions. In order to demonstrate that the velocity components display the correct behaviour at the blade surfaces, the convergence properties of these series need to be considered. Terms in the m summations which are of order $(mB)^{-1}$ are expected to lead to divergent series, or series which do not converge uniformly. The manipulations performed below are aimed at identifying those terms. Furthermore, within this group of terms, we wish

to isolate a series for which the k summation can be done analytically and for which the m summation does not converge uniformly for all values of the ζ co-ordinate. It can be anticipated that such series produce the discontinuities in the surface quantities which occur as changes in ζ are made which correspond to crossing a blade surface. For the remainder of this section our attention is confined to points within the blade row, i.e. for $0 \leqslant z \leqslant c_a$.

The identification of the discontinuous terms in the expressions for the surface velocity components depends on the evaluation of the doubly infinite series $S(r, \zeta)$ defined by

$$S(r,\zeta) = \frac{B}{\pi}\frac{1}{(\omega r_T/U)^2}\int_{r_H}^{r_T}\sum_{m=1}^{\infty}\sum_{k=1}^{\infty} R_{mBk}(\sigma)\,R_{mBk}(\sigma_0)\frac{\sin(mB\zeta)}{mB} \times\left[\frac{1}{\beta^2}+\beta^2(\lambda_{mBk}/mB)^2\right]^{-1} f(r_0)\,dr_0. \quad (60)$$

Substituting (21) for λ_{mBk} in the bracketed factor, adding and subtracting the quantity $(\omega r_0/U)^2/[1+(\omega r_0/U)^2]$ to this factor, and doing the r_0 integration term by term, the function $S(r, \zeta)$ becomes

$$\begin{aligned} S(r,\zeta) = {} & \frac{B}{\pi}\sum_{m=1}^{\infty}\frac{\sin(mB\zeta)}{mB}\sum_{k=1}^{\infty} R_{mBk}(\sigma)\int_h^1 R_{mBk}(\sigma_0)\left[\frac{r_0 f(r_0)}{1+(\omega r_0/U)^2}\right]\sigma_0\,d\sigma_0 \\ & +\frac{B}{\pi}\sum_{m=1}^{\infty}\sum_{k=1}^{\infty} R_{mBk}(\sigma)\frac{\sin(mB\zeta)}{mB}[(K_{mBk}/mB)^2+(\omega r_T/U)^2]^{-1}\int_{r_H}^{r_T}\frac{1}{r_T^2} \\ & \times[r_T^2-r_0^2(K_{mBk}/mB)^2][1+(\omega r_0/U)^2]^{-1}R_{mBk}(\sigma_0)f(r_0)\,dr_0. \end{aligned} \quad (61)$$

The k summation in the first line of (61) is just the Fourier–Bessel expansion for the bracketed function in terms of the radial eigenfunctions. Performing this summation and using the equation satisfied by the radial eigenfunctions (24) to substitute in the second integral, $S(r, \zeta)$ can be written

$$\begin{aligned} S(r,\zeta) = {} & \frac{rf(r)}{1+(\omega r/U)^2}\frac{B}{\pi}\sum_{m=1}^{\infty}\frac{\sin(mB\zeta)}{mB}+\frac{B}{\pi}\sum_{m=1}^{\infty}\sum_{k=1}^{\infty} R_{mBk}(\sigma)\frac{\sin(mB\zeta)}{(mB)^3} \\ & \times[(K_{mBk}/mB)^2+(\omega r_T/U)^2]^{-1}\int_{r_H}^{r_T}\frac{d}{dr_0}\left(r_0\frac{dR_{mBk}}{dr_0}\right)\frac{f(r_0)\,r_0}{1+(\omega r_0/U)^2}\,dr_0. \end{aligned} \quad (62)$$

Now, the eigenvalues K_{mBk} are all greater than mB, being $O(mB)$ for large mB, and the remaining integral can be integrated by parts to give

$$\begin{aligned} & \int_{r_H}^{r_T}\frac{d}{dr_0}\left(r_0\frac{dR_{mBk}}{dr_0}\right)\left[\frac{f(r_0)\,r_0}{1+(\omega r_0/U)^2}\right]dr_0 \\ & \qquad = \frac{f(r_0)\,r_0^2}{1+(\omega r_0/U)^2}\frac{dR_{mBk}}{dr_0}\bigg|_{r_H}^{r_T}-\int_{r_H}^{r_T}\frac{dR_{mBk}}{dr_0}r_0\frac{d}{dr_0}\left[\frac{f(r_0)\,r_0}{1+(\omega r_0/U)^2}\right]dr_0. \end{aligned} \quad (63)$$

The integrated term vanishes because each radial eigenfunction identically satisfies the boundary conditions at the duct walls. Another integration by parts could be done but it does not appear worth while. The important point to make is that each m, k term of the double series in (62) is at most of order $(mB)^{-2}$. Here again this series is then a regular series, and the first series in (62) is the only remaining contribution to

$S(r,\zeta)$ which could contain a discontinuity; it is proportional to the Fourier series expansion of the generalized function, ζ_j, which is defined by

$$\zeta_j = \zeta - (2j+1)\pi/B, \quad \frac{2\pi j}{B} \leqslant \zeta \leqslant \frac{2\pi}{B}(j+1), \quad j = 0, 1, \ldots, B-1. \tag{64}$$

This function was used by Reissner (1937) in his representation of a propeller wake. It has a jump of $-2\pi/B$ as ζ crosses a blade location, moving in the direction of increasing ζ.

It can be shown that the Fourier series representation of ζ_j is

$$\zeta_j = -2\sum_{m=1}^{\infty} \frac{\sin(mB\zeta)}{mB}. \tag{65}$$

With these results, the expression for $S(r,\zeta)$ becomes

$$S(r,\zeta) = -\left(\frac{B}{2\pi}\right)\zeta_j \frac{rf(r)}{1+(\omega r/U)^2} - \frac{B}{\pi}\sum_{m=1}^{\infty}\sum_{k=1}^{\infty} R_{mBk}(\sigma)\frac{\sin(mB\zeta)}{(mB)^3}$$
$$\times [(K_{mBk}/mB)^2 + (\omega r_T/U)^2]^{-1}\int_{r_H}^{r_T} r_0 \frac{dR_{mBk}}{dr_0}\frac{d}{dr_0}\left[\frac{f(r_0)\,r_0}{1+(\omega r_0/U)^2}\right]dr_0. \tag{66}$$

Using the above form for the generic series $S(r,\zeta)$, the specific series in each of the expressions for the velocity components are evaluated. First, we wish to show that, in the thickness case, v_s is continuous across the blade surfaces. This demonstration also provides a check on the assumption that the blades are locally unloaded by virtue of the relationship between p and v_s.

6.1. *Blade surface velocity components in thickness problem*

The first step in examining the value of v_s at the blade surfaces is to carry out an integration by parts in the integral over z_0. After the first integration by parts the expression for v_s is

$$v_s = \frac{BU}{2\pi\beta^2 r_T^2[1+(\omega r/U)^2]^{\frac{1}{2}}}\int_{r_H}^{r_T}\left\{\frac{2}{1-h^2}\int_0^{c_a}\frac{\partial}{\partial z_0}[t(r_0,z_0)]\,H(z-z_0)\,dz_0\right.$$
$$-\frac{1}{2}\sum_{m=-\infty}^{\infty}\sum_{k=1}^{\infty} R_{mBk}(\sigma)\frac{R_{mBk}(\sigma_0)}{\omega\lambda_{mBk}/U}\,e^{imB\zeta}\left[\left.\frac{\partial t}{\partial z_0}\right|_{z_0=0}\exp(\Lambda^{+}_{mBk}z)\right.$$
$$\left.\left.-\left.\frac{\partial t}{\partial z_0}\right|_{z_0=c_a}\exp[\Lambda^{-}_{mBk}(z-c_a)] + \int_0^{c_a}\exp[\Lambda^{\pm}_{mBk}(z-z_0)]\frac{\partial^2 t}{\partial z_0^2}\,dz_0\right]\right\}$$
$$\times[1+(\omega r_0/U)^2]^{\frac{1}{2}}\,dr_0. \tag{67}$$

The coefficients in the series containing $\partial t/\partial z_0$ are inversely proportional to λ_{mBk} which is $O(mB)$, but the exponential factors in these terms prevent the series from diverging, except as the leading or trailing edges are approached. There, unless the slope of the thickness profile vanishes, the series diverge. The divergence of these series produces the singularities in the pressure which typically occur at the leading and trailing edges of subsonic airfoils. The divergence of the surface pressure at these points is evident in the original results of McCune (1958*a*, *b*), as well as in the surface pressure results accompanying the thickness-induced camber lines presented by Erickson *et al.* (1971).

Each integration by parts over z_0 introduces another factor of $(mB)^{-1}$ in successive

terms of the double series. The second integration by parts yields integrated terms which are proportional to $\partial^2 t/\partial z_0^2$, evaluated at $z_0 = 0$, z, and c_a. These terms are $O[(mB)^{-2}]$ and so the corresponding series are uniformly convergent. Hence, away from the leading and trailing edges, all the series in v_s are uniformly convergent for all values of ζ, including those at the blade surfaces. It can therefore be concluded that v_s and p are continuous across these surfaces. The same is not true of v_n, however, which must be discontinuous at $\zeta = 2j\pi/B$ by an amount dictated by the boundary condition (39).

We have already evaluated the v_s contribution to the expression given for v_n in (46), and shown it to be continuous. Any discontinuity in v_n must then come from the $\partial\phi/\partial\zeta$ contribution. After performing a single integration by parts on the z_0 integral in the expression for $\partial\phi/\partial\zeta$ and combining the result with (46 *b*) to obtain v_n, the result is

$$
\begin{aligned}
v_n = & -\frac{B}{2\pi}\zeta_j \Delta v_n(r,z) - \frac{BU}{\pi r}[1+(\omega r/U)^2]^{\frac{1}{2}} \sum_{m=1}^{\infty}\sum_{k=1}^{\infty} \frac{R_{mBk}(\sigma)}{[(K_{mBk}/mB)^2+(\omega r_T/U)^2]} \\
& \times \frac{\sin(mB\zeta)}{(mB)^3}\int_{r_H}^{r_T} r_0 \frac{dR_{mBk}}{dr_0}\frac{d}{dr_0}\left[\frac{r_0\,\partial t(z,r_0)/\partial z}{[1+(\omega r_0/U)^2]^{\frac{1}{2}}}\right] dr_0 - \frac{BU}{2\pi\beta^2 r_T^2} \\
& \times \frac{\omega r/U}{[1+(\omega r/U)^2]^{\frac{1}{2}}}\left(\frac{2}{1-h^2}\right)\int_{r_H}^{r_T}\int_0^{c_a}\frac{\partial t}{\partial z_0}[(1+(\omega r_0/U)^2]^{\frac{1}{2}} H(z-z_0)\,dz_0\,dr_0 \\
& + \frac{BU}{4\pi\beta^2 r_T^2[1+(\omega r/U)^2]^{\frac{1}{2}}}\int_{r_H}^{r_T}\sum_{m=-\infty}^{\infty}\sum_{k=1}^{\infty}\frac{R_{mBk}(\sigma_0)\,R_{mBk}(\sigma)}{(\omega/U)\,\lambda_{mBk}[(mB/\beta^2)^2+\lambda_{mBk}^2]}\,e^{imB\zeta} \\
& \times \left\{\left.\frac{\partial t}{\partial z_0}\right|_{z_0=0} T_{mBk}(r,z,0)\exp(\Lambda_{mBk}^{+}z) - \left.\frac{\partial t}{\partial z_0}\right|_{z_0=c_a} T_{mBk}(r,z,c_a)\exp[\Lambda_{mBk}^{-}(z-c_a)]\right. \\
& \left. + \int_0^{c_a}\exp[\Lambda_{mBk}^{\pm}(z-z_0)]\,T_{mBk}(r,z,z_0)\frac{\partial^2 t}{\partial z_0^2}\,dz_0\right\}[1+(\omega r_0/U)^2]^{\frac{1}{2}}\,dr_0, \qquad (68)
\end{aligned}
$$

where

$$
\begin{aligned}
T_{mBk}(r,z,z_0) = & -\frac{1}{\omega r/U}\left[\frac{(mB)^2}{\beta^2} - imB\lambda_{mBk}\operatorname{sgn}(z-z_0)\right] \\
& + \frac{\omega r}{U}\left[\frac{M^2(mB)^2}{\beta^4} + imB\lambda_{mBk}\operatorname{sgn}(z-z_0) + \lambda_{mBk}^2\right]. \qquad (69)
\end{aligned}
$$

The first term in v_n is obtained by identifying the series representation of the generalized function ζ_j and contains the symmetric discontinuity which should occur in v_n. It makes no contribution to the continuous part of v_n, nor does the second term when evaluated at the blade surfaces. The remaining terms, which represent the continuous part of v_n or the slope of the thickness-induced camber lines, are uniformly convergent away from the leading and trailing edges. The third term in the above expression comes from the $n = 0, k = 0$ term omitted from previous treatments of the thickness problem. The camber line calculations of Erickson *et al.* (1971) and the surface pressure calculations of McCune (1958*a*, *b*) should be corrected for the presence of these terms. They make no contribution to the disturbance field upstream or downstream of the blade row and, therefore, the acoustic calculations done with this analysis (Lordi 1971) are unaffected by their inclusion.

6.2. *Blade surface velocity components in loading problem*

The blade-surface properties of the solution for the velocity field of a lifting rotor can be examined as was done for a non-lifting rotor, although the loading case is somewhat more complicated because of the presence of the trailing vortex wakes. Again the streamwise, normal, and radial components, v_s, v_n and v_r, are considered. First the behaviour of v_s is treated, followed by v_r, with v_n done last.

Since v_s is proportional to p, it must contain a discontinuity across the blade surfaces which is in the same proportion to the blade loading, Δp. Therefore, showing that the solution for the pressure field contains the correct discontinuity is equivalent to demonstrating the proper behaviour of v_s at the blade surface. Again this is done by ordering the series expansions in $(mB)^{-1}$ and, in particular, isolating a series for which the k summation can be done and for which the m summation yields the generalized function ζ_j.

As before, the first operation on the expression for p is to perform an integration by parts on the z_0 integral. The result, after some rearrangement and identification of the discontinuous terms, is

$$
\begin{aligned}
p = {} & \frac{B}{2\pi}\Delta p(r,z)\,\zeta_j - \frac{B}{\pi}\sum_{m=1}^{\infty}\sum_{k=1}^{\infty}\frac{R_{mBk}(\sigma)\sin(mB\zeta)}{(mB)^3\left[(K_{mBk}/mB)^2+(\omega r_T/U)^2\right]} \\
& \times\int_{r_H}^{r_T} R_{mBk}(\sigma_0)\frac{\partial}{\partial r_0}\left[r_0\frac{\partial}{\partial r_0}\Delta p(r_0,z)\right]dr_0 + \frac{\omega B}{2\pi\beta^2\bar{U}}\int_0^{c_a}\overline{\Delta p}(z_0)\,H(z-z_0)\,dz_0 \\
& + \frac{B}{4\pi\beta^2 r_T^2}\int_{r_H}^{r_T}\sum_{m=-\infty}^{\infty}\sum_{k=1}^{\infty}\frac{R_{mBk}(\sigma)\,R_{mBk}(\sigma_0)}{\omega\lambda_{mBk}/U}\,e^{imB\zeta} \\
& \times\left\{\Delta p(r_0,0)\frac{V_{m,k}(r_0,z,0)}{\Lambda^{+}_{mBk}}\exp\left[\Lambda^{+}_{mBk}z\right] - \Delta p(r_0,c_a)\frac{V_{m,k}(r_0,z,c_a)}{\Lambda^{-}_{mBk}}\exp\left[\Lambda^{-}_{mBk}(z-c_a)\right]\right. \\
& \left. + \int_0^{c_a}\frac{V_{m,k}(r_0,z,z_0)}{\Lambda^{\pm}_{mBk}}\exp\left[\Lambda^{\pm}_{mBk}(z-z_0)\right]\frac{\partial}{\partial z_0}\left[\Delta p(r_0,z_0)\right]dz_0\right\}dr_0. \qquad (70)
\end{aligned}
$$

The term containing the generalized function ζ_j is the term which contains the discontinuity in p; all of the remaining terms converge uniformly for all ζ away from the leading or trailing edge and, hence, are continuous across the blade surfaces. However, at the leading or trailing edge, one of the exponential factors in the integrated terms in braces approaches unity, and the series can diverge. At the trailing edge Δp should vanish according to the Kutta condition, and the convergence properties of the series in p depend on the behaviour of Δp as $z \to c_a$. At the leading edge, the linearized analysis contains a singularity in the loading, and so the series can be expected to diverge there. When the first two terms are omitted, this expression for p is valid upstream ($z < 0$) and downstream ($z > c_a$) of the blade row. Thus, away from the leading and trailing edges, p (and hence v_s) is continuous in these regions and, in particular, across the blade wakes.

Next, the properties of the expression for the radial velocity are examined, focusing on the terms due to the trailing vortex wakes. The radial velocity is tangential to the wake surfaces and should be discontinuous across them. This behaviour can be demon-

strated simply, if we consider points far downstream of the rotor where all other terms except the wake term have decayed and (59) becomes

$$v_r(z\to+\infty)=\frac{B}{\pi\rho_\infty U r_T^2}\int_{r_H}^{r_T}\int_0^{c_a}\sum_{m=1}^{\infty}\sum_{k=1}^{\infty}R'_{mBk}(\sigma)\,R_{mBk}(\sigma_0)\frac{\sin(mB\zeta)}{mB}$$
$$\times\frac{K_{mBk}}{\omega r_T/U}\left[\frac{1}{\beta^2}+\beta^2(\lambda_{mBk}/mB)^2\right]^{-1}\left[\frac{1+(\omega r_0/U)^2}{\omega r_0/U}\right]\Delta p(r_0,z_0)\,dz_0\,dr_0. \quad (71)$$

Again using the series $S(r,\zeta)$ to identify the discontinuous terms and introducing the blade circulation Γ which is defined by

$$\Gamma(r)=\int_0^c\gamma(r,s)\,ds, \quad (72)$$

where $\gamma(r,s)$ is the local vortex strength,

$$\gamma(r,s)=\Delta v_s=v_s(\zeta=2\pi j^-/B)-v_s(\zeta=2\pi j^+/B), \quad (73)$$

then

$$v_r(z\to+\infty)=\frac{B}{2\pi}\zeta_j\frac{d\Gamma}{dr}-\frac{B}{\pi\rho_\infty U}\int_0^{c_a}\sum_{m=1}^{\infty}\sum_{k=1}^{\infty}\frac{R'_{mBk}(\sigma)\,(K_{mBk}/r_T)}{[(K_{mBk}/mB)^2+(\omega r_T/U)^2]}$$
$$\times\frac{\sin(mB\zeta)}{(mB)^3}\int_{r_H}^{r_T}\frac{\partial}{\partial r_0}\left[r_0\frac{\partial}{\partial r_0}\Delta p(r_0,z_0)\right]R_{mBk}(\sigma_0)\,dr_0. \quad (74)$$

The ζ_j term produces the expected discontinuity in v_r across the wakes while the second term is continuous. Forming the difference in v_r across the blade wake locations according to the same convention adopted for Δv_s, we get

$$\Delta v_r=d\Gamma/dr. \quad (75)$$

Notice that in this convention Γ is negative when Δp is positive and work is done on the fluid.

The final task of this section is to develop further the expression for the normal component of the perturbation velocity. The terms in v_n' (recall that the prime denotes that the blade force term is omitted) which represent the wake terms are labelled $(v_n)_w$ and may be written

$$(v_n)_w=\frac{B}{2\pi r_T^2\rho_\infty U_R}\frac{1+(\omega r/U)^2}{r}\int_{r_H}^{r_T}\int_0^{c_a}\sum_{m=-\infty}^{\infty}{}'\sum_{k=1}^{\infty}R_{mBk}(\sigma)\,R_{mBk}(\sigma_0)\,e^{imB\zeta}$$
$$\times H(z-z_0)\left[\frac{1}{\beta^2}+\beta^2(\lambda_{mBk}/mB)^2\right]^{-1}\left[\frac{1+(\omega r_0/U)^2}{(\omega r_0/U)^2}\right]\Delta p(r_0,z_0)\,r_0\,dz_0\,dr_0, \quad (76)$$

where the prime on the m summation denotes that there is no $m=0$ term. The k summation can be rearranged using the same techniques employed to evaluate the series function $S(r,\zeta)$. This time the corresponding m summation can be evaluated, if the appropriate $m=0$ term is added and subtracted, in terms of the series representation of a sequence of delta functions rather than the generalized function ζ_j. When this is done the delta function terms so represented precisely cancel the blade-force term in v_n represented as a volume distribution of dipoles. The resulting expression

for v_n, which now converges everywhere except near the leading or trailing edges, is

$$
\begin{aligned}
v_n = {} & \frac{\omega B}{2\pi\beta^2 U}\left(\frac{\omega r}{U}\right)\frac{1}{\rho_\infty U_R}\int_0^{c_a}\overline{\Delta p}(z_0)\,H(z-z_0)\,dz_0 \\
& -\frac{B}{2\pi\rho_\infty U_R r}\left[1+(\omega r/U)^2\right]\int_0^{c_a}\Delta p(r,z_0)\,H(z-z_0)\,dz_0 \\
& +\frac{B}{2\pi\rho_\infty U_R r}\left[1+(\omega r/U)^2\right]\int_0^{c_a}\sum_{m=-\infty}^{\infty}{}'\sum_{k=1}^{\infty}\frac{R_{mBk}(\sigma)\,e^{imB\zeta}H(z-z_0)}{(mB)^2\left[(K_{mBk}/mB)^2+(\omega r_T/U)^2\right]} \\
& \times\int_{r_H}^{r_T}R_{mBk}(\sigma_0)\frac{\partial}{\partial r_0}\left[r_0\frac{\partial}{\partial r_0}\Delta p(r_0,z_0)\right]dr_0\,dz_0 \\
& +\frac{B}{4\pi\beta^2 r_T^2\rho_\infty U_R}\int_{r_H}^{r_T}\sum_{m=-\infty}^{\infty}\sum_{k=1}^{\infty}\frac{R_{mBk}(\sigma)\,R_{mBk}(\sigma_0)}{\omega\lambda_{mBk}/U}\,e^{imB\zeta}V_{m,k}(r_0,z,z_0) \\
& \times\left\{\frac{\omega r}{U}-\frac{imB}{\Lambda^{\pm}_{mBk}}\left[(1/r)\left(1+\omega^2 r^2/U^2\right)\right]\right\}\exp\left[\Lambda^{\pm}_{mBk}(z-z_0)\right]\Delta p(r_0,z_0)\,dz_0\,dr_0. \qquad (77)
\end{aligned}
$$

The terms on the last two lines can be integrated by parts and then manipulated using the techniques of this section to demonstrate that v_n is continuous across the blade surfaces, as it should be. The expression given above for v_n is the starting point for our development (Homicz & Lordi 1979) of the governing integral equation in the direct lifting-surface theory of a compressor rotor.

7. Equivalence of the dipole and vortex representations of the lifting surface

The pressure dipole representation of the lifting rotor flow field, which has been used in the present work, can be shown to be equivalent to the vortex representation used by Okurounmu & McCune (1970). In order to show this, the present dipole representation is re-interpreted as a vortex representation, to which it must be equivalent. The resulting vortex representation is then shown to be the same as that of Okurounmu & McCune (1970).

First, the velocity potential of a lifting rotor is written in terms of the pressure perturbation as follows:

$$\phi = -\int_{-\infty}^{z}\frac{p(z',\zeta,r)}{\rho_\infty U}dz'. \qquad (78)$$

Substituting for p from (49) and interchanging the order of integration,

$$\phi = -\frac{1}{\rho_\infty U}\int_{S_B}\Delta p(r_0,z_0)\int_{-\infty}^{z}p_D(r,\zeta,z';r_0,\zeta_0,z_0)\,dz'\,dS_B. \qquad (79)$$

Introducing the bound vorticity, γ defined in (73),

$$\phi = \int_{S_B}\gamma(r_0,z_0)\left[1+(\omega r_0/U)^2\right]^{\frac{1}{2}}\int_{-\infty}^{z}p_D\,dz'\,dS_B. \qquad (80)$$

Now it can further be shown that

$$\int_{-\infty}^{z}p_D(z',\zeta,r;z_0,r_0,\zeta_0)\,dz' = \int_{z_0}^{\infty}p_D(z,\zeta,r;z_0',\zeta_0,r_0)\,dz_0'. \qquad (81)$$

If we recognize that p_D is mathematically equivalent to the potential due to a fluid doublet ϕ_d and, by analogy with the development for unconfined flow (Ashley & Landahl 1965), identify the potential due to an elementary horseshoe vortex ϕ_γ with that due to the following doublet distribution,

$$\phi_\gamma = [1+(\omega r_0/U)^2]^{\frac{1}{2}} \int_{z_0}^{\infty} \phi_d(z, \zeta, r; z_0', \zeta_0, r_0)\, dz_0', \tag{82}$$

then the velocity potential due to a lifting rotor can be expressed as the superposition of these elementary vortex solutions by

$$\phi = \int_{S_B} \gamma(r_0, z_0)\, \phi_\gamma\, dS_B. \tag{83}$$

Each elementary horseshoe vortex has an infinitesimally long, radially oriented bound element located at z_0, r_0, with the pair of trailing vortex filaments lying along the helical undisturbed streamlines.

Okurounmu & McCune (1970) developed the solution for equally spaced, radially oriented vortex lines (and their associated trailing vortex wakes) which span the annulus. In order to show the equivalence between the present formulation and theirs, the present doublet (dipole) solution is used to construct, first, a horseshoe vortex solution and then the solution due to B equally spaced, radially oriented vortex lines. The desired integral of ϕ_d in (82) for ϕ_γ was evaluated in our development of the dipole representation of the rotor; see (35). The potential due to the radial vortex lines is obtained from

$$\phi_\Gamma = \sum_{j=0}^{B-1} \int_{r_H}^{r_T} \Gamma(r_0)\, \phi_\gamma(r, \zeta, z, r_0, 2\pi j/B, z_0)\, dr_0, \tag{84}$$

where Γ is the circulation at the radius r_0. The resulting expression for ϕ_Γ, after carrying out the j summation, is

$$\begin{aligned}
\phi_\Gamma = {} & \frac{1}{2\pi\beta^2 r_T^2}\left(\frac{\omega B}{U}\right)\left(\frac{2}{1-\bar{h}^2}\right)(z-z_0)\,H(z-z_0)\int_{r_H}^{r_T}\Gamma(r_0)\,r_0\,dr_0 \\
& + \frac{B}{2\pi\beta^2 r_T^2}\sum_{m=-\infty}^{\infty}{}'\sum_{k=1}^{\infty} R_{mBk}(\sigma)\, e^{imB\zeta}\,\frac{imBH(z-z_0)}{(mB)^2/\beta^4+\lambda_{mBk}^2} \\
& \times \int_{r_H}^{r_T} R_{mBk}(\sigma_0)\,\Gamma(r_0)\left[\frac{1+(\omega r_0/U)^2}{(\omega r_0/U)^2}\right] r_0\,dr_0 \\
& + \frac{B}{4\pi\beta^2 r_T^2}\sum_{m=-\infty}^{\infty}\sum_{k=1}^{\infty}\frac{R_{mBk}(\sigma)\, e^{imB\zeta}}{(\omega\lambda_{mBk}/U)\,[(mB)^2/\beta^4+\lambda_{mBk}^2]} \\
& \times \exp\left[\frac{imB}{\beta^2}\frac{\omega}{U}(z-z_0)-\frac{\omega\lambda_{mBk}}{U}|z-z_0|\right]\int_{r_H}^{r_T} R_{mBk}(\sigma_0)\,\Gamma(r_0) \\
& \times \left\{\frac{(mB)^2}{\beta^2(\omega r_0/U)}-\frac{\omega r_0}{U}\left[\frac{(mB)^2 M^2}{\beta^4}+\lambda_{mBk}^2\right]-\left[\frac{1+(\omega r_0/U)^2}{\omega r_0/U}\right] imB\lambda_{mBk}\right. \\
& \left. \times\,[2H(z-z_0)-1]\right\} dr_0.
\end{aligned} \tag{85}$$

This result for the potential due to B radial vortex lines, although in markedly different form, can be shown to be equivalent to that of Okurounmu & McCune (1970). When notational differences are accounted for, the $m = 0$ terms in the above expression for ϕ_Γ are easily shown to be identical to those in equation (8) of their

paper. The key step in demonstrating that the two results for ϕ_Γ are equivalent is in showing that the terms representing the trailing vortex wakes are the same. These are the $m \neq 0$ terms having no z dependence which are present downstream of the vortex lines. They are labelled ϕ_w and will be shown to be identical to the wake potential derived by Okurounmu & McCune (1970) from an entirely different approach.

Using (21), the terms in ϕ_w become

$$\phi_w = -\frac{B}{\pi r_T^2}\int_{r_H}^{r_T}\sum_{m=1}^{\infty}\sum_{k=1}^{\infty} R_{mBk}(\sigma)\,R_{mBk}(\sigma_0)\,\frac{\sin(mB\zeta)}{mB}\,\Gamma(r_0) \times\left[\frac{(\omega r_T/U)^2}{(K_{mBk}/mB)^2+(\omega r_T/U)^2}\right]\left[\frac{1+(\omega r_0/U)^2}{(\omega r_0/U)^2}\right] r_0\,dr_0. \quad (86)$$

Now the double summation is proportional to the series $S(r,\zeta)$ defined by (60) in the previous section. Introducing the addition and subtraction manipulation used there, ϕ_w becomes

$$\begin{aligned}\phi_w = &-\frac{B}{\pi r_T^2}\sum_{m=1}^{\infty}\sum_{k=1}^{\infty}\frac{\sin(mB\zeta)}{mB}\,R_{mBk}(\sigma)\int_{r_H}^{r_T}\Gamma(r_0)\,R_{mBk}(\sigma_0)\,r_0\,dr_0\\ &-\frac{B}{\pi r_T^2}\int_{r_H}^{r_T}\sum_{m=1}^{\infty}\frac{\sin(mB\zeta)}{mB}\sum_{k=1}^{\infty}R_{mBk}(\sigma_0)\,R_{mBk}(\sigma)\\ &\times\frac{\Gamma(r_0)\,[r_T^2-r_0^2(K_{mBk}/mB)^2]\,dr_0}{r_0[(K_{mBk}/mB)^2+(\omega r_T/U)^2]}. \end{aligned} \quad (87)$$

The k sum in the first line of this equation is just the Fourier–Bessel expansion for $\Gamma(r)$; the m sum is the series representation of the generalized function ζ_j. The second k summation in (87) can be identified with $d[r_0\,dS_n(r,r_0)/dr_0]/dr_0$, where $S_n(r,r_0)$ is the series defined as

$$S_n(r,r_0) = \sum_{k=1}^{\infty}\frac{R_{nk}(K_{nk}\sigma)\,R_{nk}(K_{nk}\sigma_0)}{(K_{nk}/r_T)^2+(\omega n/U)^2} \quad (88)$$

and $n = mB$. Making these substitutions,

$$\phi_w = \frac{B}{2\pi}\Gamma(r)\,\zeta_j - \frac{B}{\pi r_T^2}\sum_{m=1}^{\infty}\frac{\sin(mB\zeta)}{mB}\int_{r_H}^{r_T}\Gamma(r_0)\,\frac{d}{dr_0}\left(r_0\frac{dS_{mB}}{dr_0}\right)dr_0. \quad (89)$$

The series in (88) has been summed by Salaun (1974) and the result is given in appendix B. The next step in the derivation of ϕ_w is to integrate by parts in the second term of (89) and use the results given in (B 5) for S_n. Since its derivative vanishes at the duct walls and it is symmetric in r and r_0, we get

$$\begin{aligned}\phi_w = &\frac{B}{2\pi}\Gamma(r)\,\zeta_j + \frac{B}{\pi r_T^2}\sum_{m=1}^{\infty}\frac{\sin(mB\zeta)}{mB}\\ &\times\Bigg\{c_1(\sigma_{mB})\int_{\sigma_{mBH}}^{\sigma_{mB}}\sigma_{mB_0}\frac{d\Gamma}{d\sigma_{mB_0}}I'_{mB}(\sigma_{mB_0})\,d\sigma_{mB_0}\\ &+c_2(\sigma_{mB})\int_{\sigma_{mBH}}^{\sigma_{mB}}\sigma_{mB_0}\frac{d\Gamma}{d\sigma_{mB_0}}K'_{mB}(\sigma_{mB_0})\,d\sigma_{mB_0}\\ &+c_3(\sigma_{mB})\int_{\sigma_{mB}}^{\sigma_{mBT}}\sigma_{mB_0}\frac{d\Gamma}{d\sigma_{mB_0}}I'_{mB}(\sigma_{mB_0})\,d\sigma_{mB_0}\\ &+c_4(\sigma_{mB})\int_{\sigma_{mB}}^{\sigma_{mBT}}\sigma_{mB_0}\frac{d\Gamma}{d\sigma_{mB_0}}K'_{mB}(\sigma_{mB_0})\,d\sigma_{mB_0}\Bigg\}, \end{aligned} \quad (90)$$

where $\sigma_{mB} = mB\omega r/U$ and the primes denote differentiation with respect to the argument. After rearranging the ranges of the integrals between σ_{mB_H} and σ_{mB_T}, the terms in braces can be identified with $-r_T^2\,\chi_{mB}$, where χ_{mB} is the wake function defined by Okurounmu & McCune (1970). Accounting for the difference in blade locations (theirs are at $((2j+1)\pi)/B$, which introduces a $(-1)^m$ factor), the above result for ϕ_w is then equivalent to theirs.

It remains to be shown that the $m \neq 0$ terms in (85) which contain the exponential factors in $z - z_0$ are the same as the corresponding terms in (8) of Okurounmu & McCune (1970). This part of the demonstration requires the identification of the radial integrals

$$\int_h^1 \Gamma(\sigma_0)\, R_{mBk}(\sigma_0)\, \sigma_0\, d\sigma_0,$$

$$\int_h^1 \frac{\Gamma(r_0)\,[r_T^2 - r_0^2\,(K_{mBk}/mB)^2]}{r_0^2\,[(K_{mBk}/mB)^2 + (\omega r_T/U)^2]}\, R_{mBk}(\sigma_0)\, \sigma_0\, d\sigma_0$$

as the coefficients of $R_{mBk}(\sigma)$ in the Fourier–Bessel expansions of the bound vorticity Γ, and the wake function χ_{mB} respectively. The latter step follows from the above demonstration that the k series beginning on the second line of (87) is indeed proportional to χ_{mB}. The required identifications can be made if the factors in braces in (85) are rearranged using the addition and subtraction manipulation of the previous section. Then, having demonstrated that the fundamental singularity solutions used here are equivalent to those used by Okurounmu & McCune (1970), we have concluded that the expressions constructed from them for the rotor-loading flow fields are also.

8. Sample numerical results

Two examples have been selected to illustrate numerical evaluations of the expressions derived here. In the first, calculations of thickness-induced camber lines are discussed. In the second, lifting-surface results for the blade loading are presented and compared with the corresponding strip-theory values.

8.1. *Thickness-induced camber lines*

As first pointed out by McCune (1958*a*) and discussed here in § 2, the effects of blade thickness and blade loading may be treated separately if the thickness is distributed about camber lines which cause the local blade loading to vanish. These thickness-induced camber lines may be computed by evaluating the expression given in (68) for the thickness contribution to the normal velocity component.

When evaluated at the blade surface, the continuous part of v_n is proportional to the slope of the camber line (see (37) and (38)). As discussed below (68), the third term, which originates from the $n = 0, k = 0$ term in the revised source solution, was omitted in the thickness-induced camber-line computations by Erickson *et al.* (1971). The contribution of this term has been evaluated for one of their examples so that the significance of the correction can be seen.

The case considered for evaluation has a nearly sonic inflow at the blade tips ($M_R = 0{\cdot}98$). The rotor has 64 blades, a hub-to-tip ratio of 0·9 and a value of c_a/r_T of 0·049. Each blade has a symmetric parabolic-arc chordwise thickness distribution. The maximum thickness-to-chord ratio decreases somewhat from a value of τ_H at

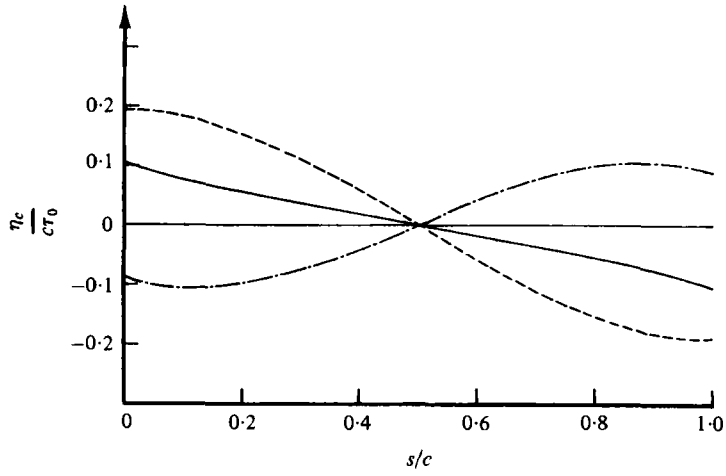

FIGURE 3. Thickness-induced camber line for parabolic-arc profile. —·—, Previous result (Erickson, Lordi & Rae 1971); – – –, correction term introduced in present paper; ——, corrected thickness-induced camber line. The parameters were $B = 64$, $h = 0{\cdot}9$, $c_a/r_T = 0{\cdot}049$, $M = 0{\cdot}6$, $M_T = 0{\cdot}775$, $M_R = 0{\cdot}98$, $r/r_T = 1$.

the hub to $0{\cdot}8\tau_H$ at the tips. The blade ordinates computed at the tip radius are shown in figure 3, normalized by the local blade chord c and a reference thickness ratio τ_0. (Previous treatments of the thickness problem used an incorrect weighting factor in the integration over radius. If the radial distribution of thickness is reinterpreted so that the integrals evaluated are correct, then τ_0 is not the thickness ratio at the hub, as stated in the earlier work, but the ratio of the maximum thickness at the hub to the axial chord projection.) In figure 3, the result reported by Erickson *et al.* (1971) is shown along with the correction derived here and the net result. It can be seen that the correction due to the revision of the source solution actually brings about a change in sign of the induced incidence part of the blade ordinate. The sign of the revised result for the induced incidence agrees with that computed for simple source–sink representations of a cascade of non-lifting blades (Erickson, private communication).

The blade pressure distribution is also affected by the revision of the source solution, but not as significantly as the camber line. The correction to the pressure is proportional to the thickness distribution; it vanishes at the leading and trailing edges and is symmetric about the midchord. The essential character of the thickness part of the subsonic pressure distribution, which is singular at the leading and trailing edges, is unchanged.

8.2. *Lifting-surface calculations*

Starting from the expression given in (77) for the loading contribution to the normal velocity component, Homicz & Lordi (1979) have developed a lifting-surface analysis for the flow through an annular blade row. One of the numerical evaluations of that theory which best demonstrates the three-dimensional effects is presented here. In the case considered, the rotor blades are thin flat plates, twisted so that the angle of attack is 5° at each radial station. The number of blades is 30, the hub-to-tip ratio is 0·5, and the ratio c_a/r_T is 0·1. The axial Mach number is 0·5 and, at the blade tips, the relative Mach number of the inflow is 0·707. The results obtained for the sectional

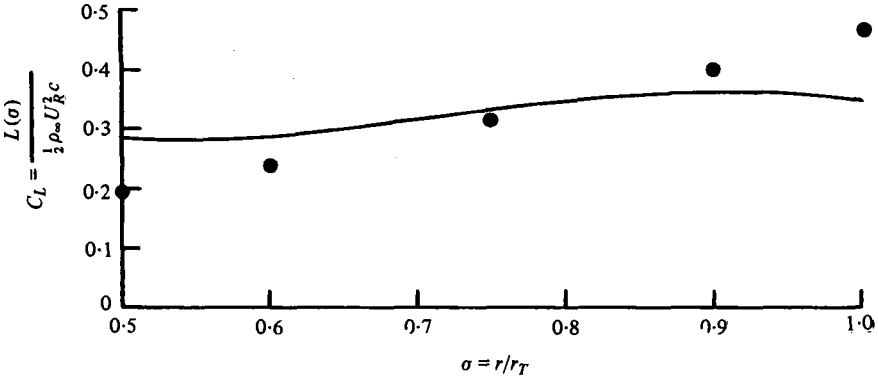

FIGURE 4. Lifting-surface results for flat plates at an angle of attack of 5°. ——, 3-D theory; ●, 2-D theory. The parameters were $B = 30$, $h = 0{\cdot}5$, $c_a/r_T = 0{\cdot}1$, $M = 0{\cdot}5$, $M_T = 0{\cdot}5$, $M_R = 0{\cdot}707$.

lift-coefficient, defined as the lift divided by $\frac{1}{2}\rho_\infty U_R^2 c$, are shown in figure 4. The results of a strip-theory calculation are shown for comparison. The strip theory provides a good approximation at mid-annulus, but substantially underestimates the loading near the hub and overestimates it near the tips. The difference in the behaviour of the three-dimensional and strip-theory results is a consequence of the trailing vorticity, which tends to reduce spanwise variations. This feature of the three-dimensional theory is discussed in more detail by Homicz & Lordi (1979) and also by McCune & Dharwadkar (1972), who treated the lifting-line limit.

9. Summary

The linearized solution for the three-dimensional, compressible flow through an annular blade row has been reviewed. Revisions have been made in singularity solutions superimposed to represent the blade thickness and loading contributions to the rotor flow field. A term previously omitted from the solution for a mass source affects the blade surface pressure distributions (McCune 1958*a*, *b*) and thickness-induced camber lines (Erickson *et al.* 1971) presented previously for subsonic relative tip speeds. While the general character of the subsonic pressure distributions is unchanged, the computed corrections to the thickness-induced camber lines are more significant. For the case illustrated in the previous section, the correction results in a change of sign in the induced incidence part of the blade ordinate.

The revised source solution has been used to form a pressure dipole solution, which in turn has been used to construct the rotor-loading contribution to the flow field. The present pressure-dipole representation of the lifting surface has been shown to be equivalent to the vortex representation of Okurounmu & McCune (1970, 1974). A direct lifting-surface analysis (Homicz & Lordi 1979) has been based on the present formulation. An example of the three-dimensional lifting-surface calculations discussed in the previous section shows that the effect of the trailing vortex wakes is to reduce the spanwise variation of the sectional lift, in marked contrast to the corresponding strip theory. Also, direct lifting-surface calculations have been done for the same conditions specified in the inverse calculations done by Okurounmu & McCune (1974). The camber lines computed in the inverse problem were specified as input in the direct lifting-surface computations. It was reported previously (Homicz & Lordi

(1979) that good agreement was obtained for a case in which the circulation was a constant, but not for a case in which the spanwise variation was prescribed in the design calculation. Additional calculations done since have shown good agreement in both cases. It was found that, since the solidity was relatively high in these examples, collocation points had to be located closer to the trailing edge in order for our lifting-surface computations to agree with both design cases.

The present version of the dipole representation of a lifting surface in steady flow differs from that of Namba (1972). The differences in the basic solution for the pressure field result from the revision of the dipole solution reported here, and also from a radially dependent scale factor which he introduced into the superposition of the dipole solutions. We have concluded on the basis of the formal development presented here that this scale factor should not be included.

The work described in this paper was supported by the Air Force Aero-Propulsion Laboratory under Contract F33615-73-C-2046. The authors wish to thank Drs J. C. Erickson, Jr, J. P. Nenni and W. J. Rae for helpful discussions held during the course of this work.

Appendix A. Mass and momentum balances for the flow-field solutions

It has been shown that the singularity and rotor flow-field solutions give the correct mass addition rate $\dot{m}$, axial component of the net force on the fluid F_z, and axial component of the torque T_z. The control volume for which these checks were made is bounded by the duct walls and the annular areas perpendicular to the duct axis at upstream and downstream infinity. Since this control volume rotates with angular velocity ω (in the negative θ direction), the conservation laws for a non-inertial reference frame must be used. The appropriate integral forms of the equations for conservation of mass, momentum, and angular momentum for such a control volume have been taken from Shames (1962). Then, these equations have been linearized so that they are expressed in terms of the undisturbed flow properties ρ_∞, U and ωr, and the perturbation quantities p, ρ, v_r, v_θ and v_z. These equations were specialized further to account for the fact that all the flow-field solutions decay at upstream infinity and satisfy the boundary condition of no flow through the duct walls. Attention has been confined to the expressions for mass conservation and to the axial components of the momentum and angular momentum balances. Under the present set of assumptions, the expressions for $\dot{m}$, F_z, and T_z in terms of the flow field variables become

$$\dot{m} = \int_{r_H}^{r_T}\int_0^{2\pi} (\rho_\infty v_z + \rho U)|_{z\to\infty}\, r\, dr\, d\theta, \tag{A 1}$$

$$F_z = \int_{r_H}^{r_T}\int_0^{2\pi} (2\rho_\infty U v_z + \rho U^2 + p)|_{z\to\infty}\, r\, dr\, d\theta, \tag{A 2}$$

$$T_z = -2\int_{-\infty}^{\infty}\int_{r_H}^{r_T}\int_0^{2\pi} \rho_\infty(\omega r v_r)\, r\, dr\, d\theta\, dz + \int_{r_H}^{r_T}\int_0^{2\pi} [\rho_\infty U r v_\theta + \omega r^2(\rho_\infty v_z + \rho U)]|_{z\to\infty}\, r\, dr\, d\theta. \tag{A 3}$$

Appendix B. Summation of the series $S_n(r, r_0)$

The series defined in (88) appears repeatedly in the expressions for the surface velocity components. Its summation in terms of modified Bessel functions, as accomplished by Salaun (1974), provides the key to demonstrating the equivalence of the dipole and vortex representations of the lifting surface. If we differentiate the series twice with respect to σ, use the Fourier–Bessel expansion for $\delta(r-r_0)$, and introduce the notation $\sigma_n = n\omega r/U$ then the following differential equation is obtained for S_n:

$$\frac{1}{\sigma_n}\frac{d}{d\sigma_n}\left(\sigma_n \frac{dS_n}{d\sigma_n}\right) - [(n/\sigma_n)^2 + 1]\, S_n = -r_T^2 \frac{\delta(\sigma_n - \sigma_{n_0})}{\sigma_n}. \tag{B 1}$$

This equation is solved subject to the hard-wall boundary conditions, i.e., that $dS_n/d\sigma_n$ vanish at the inner and outer duct walls, $\sigma_n = \sigma_{n_H}$ and σ_{n_T}. Moreover, S_n is required to be continuous at $\sigma_n = \sigma_{n_0}$ and $dS_n/d\sigma_n$ satisfies the following jump condition at $\sigma_n = \sigma_{n_0}$, which is derived by integrating the governing differential equation from $\sigma_{n_0} - \epsilon$ to $\sigma_{n_0} + \epsilon$,

$$\left[\left(\frac{dS_n}{d\sigma_n}\right)_{+}_{\sigma_{n0}} - \left(\frac{dS_n}{d\sigma_n}\right)_{-}_{\sigma_{n0}}\right] = -\frac{r_T^2}{\sigma_{n_0}}. \tag{B 2}$$

The modified Bessel functions $I_n(\sigma_n)$ and $K(\sigma_n)$ are linearly independent solutions of the homogeneous equation for S_n. For $\sigma_n < \sigma_{n_0}$, assume

$$S_n(\sigma_n, \sigma_{n_0}) = c_1(\sigma_{n_0})\, I_n(\sigma_n) + c_2(\sigma_{n_0})\, K_n(\sigma_n), \tag{B 3}$$

while, for $\sigma_n > \sigma_{n_0}$, set

$$S_n(\sigma_n, \sigma_{n_0}) = c_3(\sigma_{n_0})\, I_n(\sigma_n) + c_4(\sigma_{n_0})\, K_n(\sigma_n). \tag{B 4}$$

The solution which satisfies all of the above boundary conditions is

$$\left.\begin{aligned}
c_1 &= \frac{-r_T^2 K_n'(\sigma_{n_H})}{Z}\,[K_n'(\sigma_{n_T})\, I_n(\sigma_{n_0}) - I_n'(\sigma_{n_T})\, K_n(\sigma_{n_0})],\\
c_2 &= \frac{r_T^2 I_n'(\sigma_{n_H})}{Z}\,[K_n'(\sigma_{n_T})\, I_n(\sigma_{n_0}) - I_n'(\sigma_{n_T})\, K_n(\sigma_{n_0})],\\
c_3 &= \frac{-r_T^2 K_n'(\sigma_{n_T})}{Z}\,[K_n'(\sigma_{n_H})\, I_n(\sigma_{n_0}) - I_n'(\sigma_{n_H})\, K_n(\sigma_{n_0})],\\
c_4 &= \frac{r_T^2 I_n'(\sigma_{n_T})}{Z}\,[K_n'(\sigma_{n_H})\, I_n(\sigma_{n_0}) - I_n'(\sigma_{n_H})\, K_n(\sigma_{n_0})],
\end{aligned}\right\} \tag{B 5}$$

where

$$Z \equiv I_n'(\sigma_{n_T})\, K_n'(\sigma_{n_H}) - I_n'(\sigma_{n_H})\, K_n'(\sigma_{n_T}) \tag{B 6}$$

and the primes denote differentiation with respect to the argument.

REFERENCES

Ashley, H. & Landahl, M. 1965 *Aerodynamics of Wings and Bodies.* Addison-Wesley.

Erickson, J. C., Lordi, J. A. & Rae, W. J. 1971 On the transonic aerodynamics of a compressor blade row. *Calspan Corp. Rep.* no. AI-3003-A-1.

Homicz, G. F. & Lordi, J. A. 1979 Three-dimensional lifting-surface theory for an annular blade row. *A.S.M.E. Paper* 79-GT-182.

LORDI, J. A. 1971 Noise generation by a rotating blade row in an infinite annulus. *A.I.A.A. 4th Fluid and Plasma Dynamic Conf.*, paper 71-617. (Also Report on a study of noise generation by a rotating blade row in an infinite annulus. *Calspan Corp. Rep.* no. AI-2836-A-1.)

MCCUNE, J. E. 1958*a* A three-dimensional theory of axial compressor blade rows – application in subsonic and supersonic flows. *J. Aerospace Sci.* **25**, 544.

MCCUNE, J. E. 1958*b* The transonic flowfield of an axial compressor blade row. *J. Aerospace Sci.* **25**, 616.

MCCUNE, J. E. & DHARWADKAR, S. P. 1972 Lifting-line theory for subsonic axial compressor rotors. *MIT Gas Turbine Lab. Rep.* no. 110.

NAMBA, M. 1972 Lifting surface theory for a rotating subsonic or transonic blade row. *Aero. Res. Counc.* R.&M. 3740.

NAMBA, M. 1976 Lifting surface theory for unsteady flows in a rotating annular cascade. Proceedings of IUTAM Symposium on Aeroelasticity in Turbomachines, Paris, Oct. 1976. *Revue Française de Mécanique*, special issue, p. 39.

NAMBA, M. 1977 Three-dimensional analysis of blade force and sound generation for an annular cascade in distorted flows. *J. Sound Vib.* **50** (4), 479.

OKUROUNMU, O. & MCCUNE, J. E. 1970 Three-dimensional vortex theory of axial compressor blade rows at subsonic and transonic speeds. *A.I.A.A. J.* **8**, 1275.

OKUROUNMU, O. & MCCUNE, J. E. 1974 Lifting surface theory of axial compressor blade rows. I: Subsonic compressor. *A.I.A.A. J.* **12**, 1363. II: Transonic compressor. *A.I.A.A. J.* **12**, 1372.

REISSNER, H. 1937 On the vortex theory of the screw propeller. *J. Aero. Sci.* **5**, 1.

SALAUN, P. 1974 Unsteady aerodynamic pressure on an annular cascade in subsonic flow. *Office National d'Etudes et de Recherches Aérospatiale Publ.* no. 158. (Translated as *European Space Agency Tech. Transl.* ESA-TT-173, July 1975.)

SALAUN, P. 1976 Flutter instability in an annular cascade. Proceedings of IUTAM Symposium on Aeroelasticity in Turbomachines, Paris, Oct. 1976. *Revue Française de Mécanique*, special issue, p. 35.

SHAMES, I. 1962 *Mechanics of Fluids*. McGraw-Hill.

WU, CHUNG-HUA 1952 A general theory of three-dimensional flow in subsonic and supersonic turbomachines of axial-, radial-, and mixed-flow types. *N.A.C.A.* TN 2604.